Exploring the Higgs boson's coupling to the charm quark with the ATLAS experiment

Seminar at the University of Warwick

24th February 2022

Andy Chisholm (University of Birmingham)

This project has received funding from the European Union's Horizon 2020 research and innovation programme under grant agreement No. 714893 (ExclusiveHiggs)

Introduction and Motivation

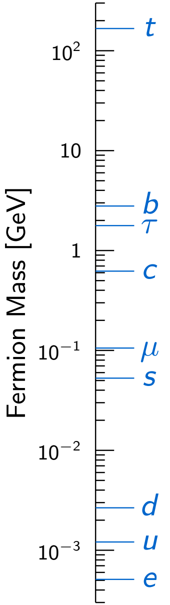

The masses of the charged fermions appear randomly chosen and span several orders of magnitude...

What is the origin of this pattern?

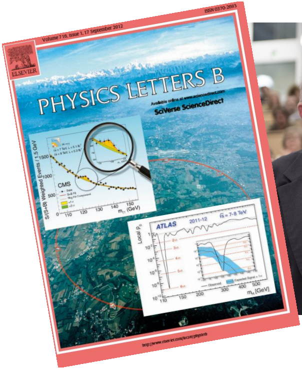

Almost ten years since the discovery of the Higgs boson and verification of the Brout-Englert-Higgs mechanism, are we any closer to fundamentally understanding fermion mass generation?

Fermion masses in the Standard Model (SM)

"Yukawa" couplings between the Higgs (ϕ) and fermion (ψ) fields are possible:

$$\mathcal{L}_{\text{fermion}} = -y_f \cdot \left[\bar{\psi}_L \phi \psi_R + \bar{\psi}_R \bar{\phi} \psi_L\right]$$

If $V(\phi)$ has a non-zero VEV, expansion leads to (h is the physical Higgs field):

$$\mathcal{L}_{\text{fermion}} = \underbrace{-\frac{y_f v}{\sqrt{2}} \cdot \bar{\psi}\psi}_{\text{mass term}} \underbrace{- \frac{y_f}{\sqrt{2}} \cdot h\bar{\psi}\psi}_{\text{coupling term}}$$

Leads to Higgs–fermion coupling proportional to the fermion mass ($y_f = \sqrt{2} m_f / v$)

- Gauge invariant fermion mass terms in SM ✓
- y_f computed in SM given knowledge of v and m_f ($v = 2M_W/g \approx 246$ GeV from EW observables) ✓
- Offers no fundamental insight into the observed fermion mass hierarchy ✗

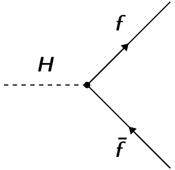

While Yukawa couplings provide concrete predictions for $Hf\bar{f}$ interactions, they fail to describe the fundamental origin of the fermion mass hierarchy...

Physics beyond the SM is clearly required to explain the fermion mass pattern!

ATLAS and CMS measurements of the Higgs boson confirm couplings to 3rd generation fermions and the muon are consistent with the SM Yukawa expectation

- Given the shortcomings of the Yukawa model, there's **no guarantee the couplings to other fermions will behave in the same way**
- **Any discrepancy could provide an important insight** into the fundamental mechanism behind the fermion mass pattern
- We must **endeavour to measure the couplings of the Higgs boson to all of the fermions**

The frontier now lies at the charm quark...

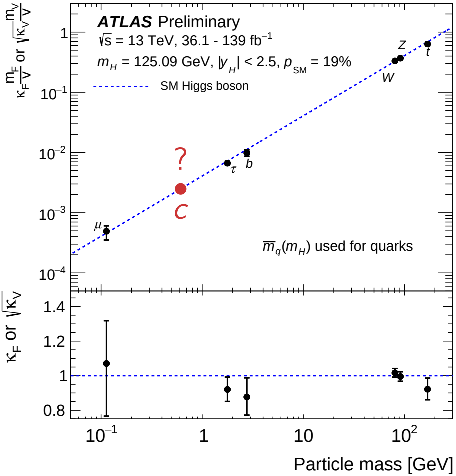

Figure from ATLAS-CONF-2021-053, annotations are my own

Why is the interaction of the Higgs boson with the charm quark interesting?

- The smallness of the SM charm quark Yukawa coupling ($\approx 4 \times 10^{-3}$) make possible **modifications from potential new physics easier to spot**
- $H \to c\bar{c}$ decays constitute one of the **largest expected contributions** to Γ_H for which we have **no experimental evidence**
- Some BSM explanations of the fermion mass spectrum could naturally lead to an **enhancement of Higgs boson couplings to the 1st and 2nd generation quarks** to the level of the SM b-quark coupling†

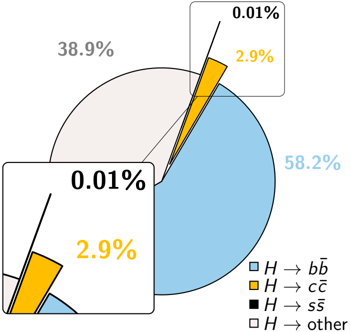

SM $m_H = 125$ GeV $H \to q\bar{q}$ branching fractions, $H \to u\bar{u}/d\bar{d}$ too small to show!

Confronting the scenario $y_c = y_b^{\text{SM}}$ (around $4.6 \times y_c^{\text{SM}}$) is an important step on the path towards testing the SM prediction!

† See for example: Phys. Rev. D 98 (2018) 055001, Phys. Rev. D 94 (2016) 115031 and Phys. Lett. B 755 (2016) 504

Several methods to study the $Hc\bar{c}$ coupling have been proposed in the literature, the ATLAS experiment has explored† three of the most promising with Run 2 data:

Idea 1 - Exclusive $H \to J/\psi\,\gamma$ decays

- The rare radiative decay $H \to J/\psi\,\gamma$ (with $J/\psi \to \mu^+\mu^-$) has been proposed as an experimentally clean probe of the $Hc\bar{c}$ coupling [Phys. Rev. D 88 (2013) 053003]

Idea 2 - Inclusive $H \to c\bar{c}$ decays

- Manifestly sensitive to the $Hc\bar{c}$ coupling, use c-jet tagging to identify decay

Idea 3 - Charm quark initiated Higgs boson production

- Contributions to $H+$jet production such as $gg \to Hg$ (via c-quark loop), $gc \to Hc$ and $c\bar{c} \to Hg$ are directly sensitive to the $Hc\bar{c}$ coupling via cross-section and kinematic features (e.g. p_T^H) [Phys. Rev. Lett. 118 (2017) 121801]

Other possibilities, not yet investigated by ATLAS:

- Direct identification of cH production [Phys. Rev. Lett. 115 (2015) 211801]
- $W^\pm H$ charge asymmetry [JHEP 02 (2017) 083]
- Constraints from global combination and limits on Γ_H [CERN-2019-007]

† **Equivalent CMS studies: 1 - Eur. Phys. J. C 79 (2019) 94, 2 - JHEP 03 (2020) 131, 3 - Phys. Lett. B 792 (2019) 369**

The radiative decay $H \to J/\psi\,\gamma$ could provide a clean probe of the $Hc\bar{c}$ coupling at the LHC

- **Interference** between **direct** ($H \to c\bar{c}$) and **indirect** ($H \to \gamma\gamma^*$) contributions
- **Direct** (upper diagram) amplitude provides sensitivity to the **magnitude and sign** of the $Hc\bar{c}$ coupling
- **Indirect** (lower diagram) amplitude provides dominant contribution to the width, not sensitive to $Hc\bar{c}$ coupling
- Very rare decays in the SM, but **rate dominated by indirect component**, sensitivity to $Hc\bar{c}$ coupling rather diluted

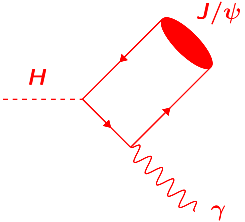

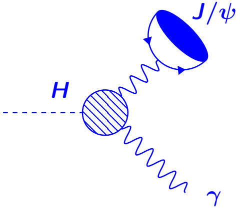

$$\Gamma \propto \left|\mathcal{A}_{\mathrm{I}} - \mathcal{A}_{\mathrm{D}} \cdot \frac{y_c}{y_c^{SM}}\right|^2$$

$$|\mathcal{A}_{\mathrm{I}}| \approx 20 \times |\mathcal{A}_{\mathrm{D}}|$$

$$\mathcal{B}\,(H \to J/\psi\,\gamma) = (3.01 \pm 0.16) \times 10^{-6}\ \dagger$$

† For more details see: Phys. Rev. D 100 (2019) 054038 (arXiv:1907.06473), JHEP 1508 (2015) 012 (arXiv:1505.03870), Phys. Rev. D 90 (2014) 113010 (arXiv:1407.6695)

ATLAS has performed a search for $H \to J/\psi\,\gamma$ with 36 fb^{-1} of 13 TeV *pp* collision data (analogous *Z* decays and $\{\psi(2S), \Upsilon(nS)\}\,\gamma$ channel also considered)

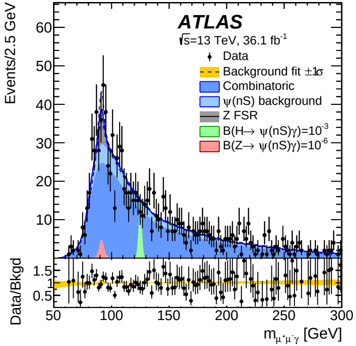

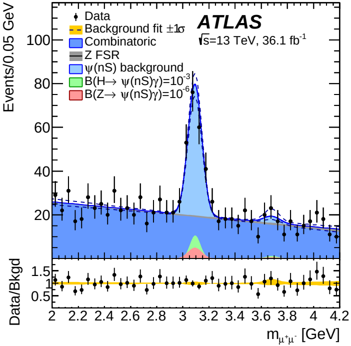

Observed 95% CL limit: $\mathcal{B}\,(H \to J/\psi\,\gamma) < 3.5 \times 10^{-4}$

- When the sensitivity is far ($\approx 100\times$) from the SM prediction, interpreting this branching fraction limit in terms of the $Hc\bar{c}$ coupling is a delicate matter†

⚠ **Can be roughly interpreted as a bound of $|y_c/y_c^{\mathrm{SM}}| < \mathcal{O}(100)$** ⚠

† **See Phys. Rev. D 100 (2019) 073013 and Phys. Rev. D 92 (2015) 033016 for more details**

Prospects for the $H \to J/\psi\,\gamma$ channel in a HL-LHC scenario with $\sqrt{s} = 14$ TeV and $3000\,\text{fb}^{-1}$ were assessed based on a projection of the original ATLAS Run 1 $H \to J/\psi\,\gamma$ result [Phys. Rev. Lett. 114 (2015) 121801]

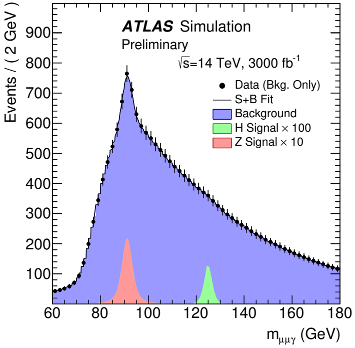

- In addition to the "cut-based" approach used in the Run 1 and 2 analyses, the sensitivity of an MVA-based event selection was considered
- The MVA-based expected 95% CL branching fraction limit was found to be: $\mathcal{B}\,(H \to J/\psi\,\gamma) < (44^{+19}_{-12}) \times 10^{-6}$
- Projected sensitivity **remains far (15×) from SM expectation** of $\mathcal{B}\,(H \to J/\psi\,\gamma) \approx 3 \times 10^{-6}$

New ideas likely required to approach SM sensitivity in a HL-LHC scenario with this channel!

Inclusive $H \to c\bar{c}$ decays are perhaps the most obvious probe of the $Hc\bar{c}$ coupling

- Compared to $H \to J/\psi\,\gamma$, a SM branching fraction of 2.9% is huge! Furthermore, the decay width scales directly with y_c^2 ✓
- Every $1\,\text{fb}^{-1}$ of $\sqrt{s} = 13$ TeV pp collision data contains around 1600 $H \to c\bar{c}$ decays ✓
- This is still orders of magnitude below the **huge** multi-jet background at the LHC... ✗

How can we mitigate the background problem?

- Charm quark initiated jets (c-jet) will typically contain a **c-hadron**, while most of the jets produced in LHC pp collisions will not
- Use **c-jet tagging algorithms** to exploit the presence of **c-hadrons** within the jets

What else can we do to help?

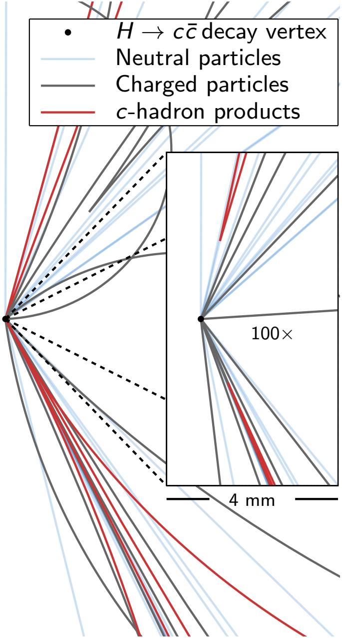

$VH, H \to c\bar{c}$ - Introduction

Focus on VH production ($V = \{W, Z\}$)

- $V \to$ leptons offer **convenient trigger strategy**
- **Enhanced S/B** w.r.t. inclusive production, particularly at high p_T^V

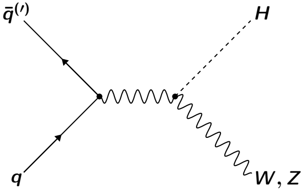

"Tried and Tested" - VH sucessfully exploited by ATLAS and CMS to observe $H \to b\bar{b}$ decays!

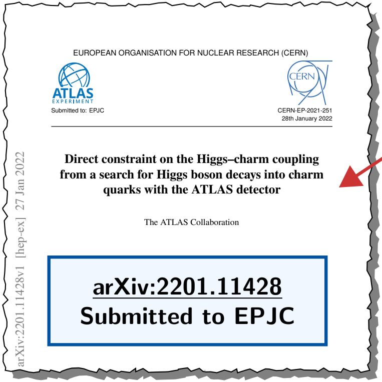
EUROPEAN ORGANISATION FOR NUCLEAR RESEARCH (CERN)

ATLAS EXPERIMENT

Submitted to: EPJC

CERN-EP-2021-251
28th January 2022

Direct constraint on the Higgs–charm coupling from a search for Higgs boson decays into charm quarks with the ATLAS detector

The ATLAS Collaboration

arXiv:2201.11428v1 [hep-ex] 27 Jan 2022

arXiv:2201.11428
Submitted to EPJC

Combine c-tagging and VH production to search for $H \to c\bar{c}$ decays with ATLAS

- New result extends earlier Run 2 analysis† based on $36\,\text{fb}^{-1}$ dataset and $Z(\ell\ell)H(c\bar{c})$ channel alone
- **Complete** ATLAS Run 2 $\sqrt{s} = 13$ TeV $139\,\text{fb}^{-1}$ pp dataset used
- **Both $Z(\ell\ell, \nu\nu)H$ and $W(\ell\nu)H$** production channels considered

† **Phys. Rev. Lett. 120 (2018) 211802**

$VH, H \to c\bar{c}$ - Event selection strategy "in a nutshell"

Strategy closely linked to ATLAS $VH, H \to b\bar{b}$ analyses and based on 3 channels, each targeting a distinct sub-mode of VH production:

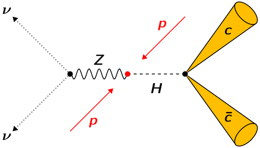

0 lepton channel

- Target the $Z(\nu\nu)H(c\bar{c})$ signature with large $E_{\mathrm{T}}^{\mathrm{miss}}$

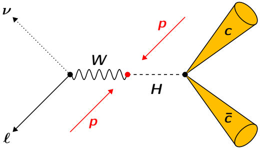

1 lepton channel

- Target the $W(\ell\nu)H(c\bar{c})$ signature with $E_{\mathrm{T}}^{\mathrm{miss}}$ and exactly one e or μ

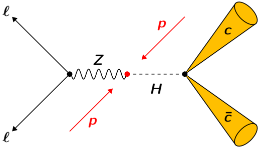

2 lepton channel

- Target the $Z(\ell\ell)H(c\bar{c})$ signature with e^+e^- or $\mu^+\mu^-$

Identify high p_{T}^{V} $VH, V \to$ leptons signature in each of these channels, in addition to at least two jets, consistent with $H \to c\bar{c}$, by means of c-jet identification

A dedicated flavour tagging working point, optimised for the $VH, H \to c\bar{c}$ search, is built from two components:

- **1)** - `DL1` (Deep NN) algorithm implemented as a c-tagger
- **2)** - `MV2c10` (BDT) b-tagger implemented as a veto at the 70% b-jet efficiency working point

Jets are "c-tagged" if both conditions are passed

- Together with a b-tag veto on non-signal jets, this ensures **orthogonality of the event selection with the $VH, H \to b\bar{b}$ analysis**

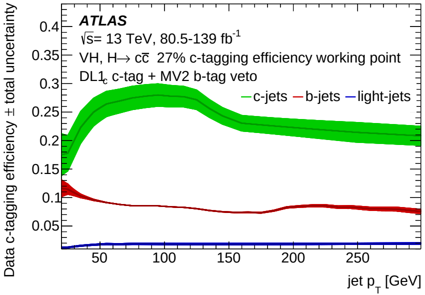

Jet Flavour Class	Efficiency (rejection)
c-jets	**27% (-)**
b-jets	**8% (13)**
Light flavour jets	**1.6% (63)**

For more details on ATLAS flavour tagging algorithms, see:

Eur. Phys. J. C 79 (2019) 970

"Truth-flavour Tagging" - To maximise the statistical power of the main background samples, events are weighted by their probability (parameterised by jet p_T, $|\eta|$ and ΔR_{jj}) of being c-tagged, as opposed to accept/reject based on `DL1` and `MV2c10` discriminants

Dedicated measurements of the *c*-tagging efficiency in data:

- Deploy baseline methods also used by ATLAS for *b*-tagging calibration
- Efficiency in data measured relative to simulation as a "scale factor" (SF) with a **typical precision of 5 - 10%**

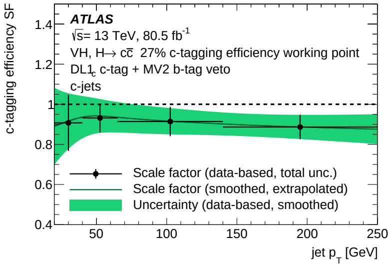

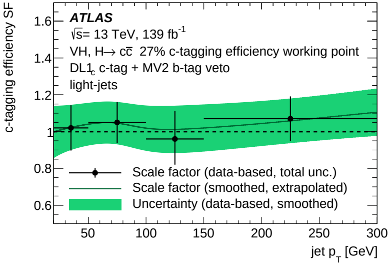

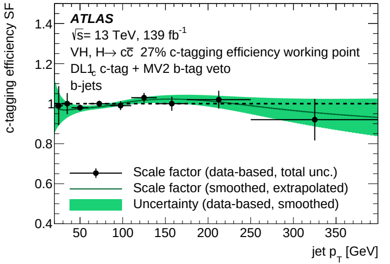

Light flavour jets - Measured with a sample of $Z+$ jet events

***c*-jets (upper) and *b*-jets (lower)** - Measured with a sample of semi-leptonic and di-leptonic $t\bar{t}$ events, respectively

Monte Carlo (MC) event generators are used to model both the $VH, H \to c\bar{c}/b\bar{b}$ signal processes and main background processes, normalised to the most accurate cross-section predictions available:

Process	ME generator	ME PDF	PS and hadronisation	Tune	Cross-section order
$qq \to VH$ $(H \to c\bar{c}/b\bar{b})$	Powheg-Box v2 + GoSam + MiNLO	NNPDF3.0NLO	Pythia 8.212	AZNLO	NNLO(QCD) +NLO(EW)
$gg \to ZH$ $(H \to c\bar{c}/b\bar{b})$	Powheg-Box v2	NNPDF3.0NLO	Pythia 8.212	AZNLO	NLO+NLL
$t\bar{t}$	Powheg-Box v2	NNPDF3.0NLO	Pythia 8.230	A14	NNLO +NNLL
t/s-channel single top	Powheg-Box v2	NNPDF3.0NLO	Pythia 8.230	A14	NLO
Wt-channel single top	Powheg-Box v2	NNPDF3.0NLO	Pythia 8.230	A14	Approx. NNLO
V+jets	Sherpa 2.2.1	NNPDF3.0NNLO	Sherpa 2.2.1	Default	NNLO
$qq \to VV$	Sherpa 2.2.1	NNPDF3.0NNLO	Sherpa 2.2.1	Default	NLO
$gg \to VV$	Sherpa 2.2.2	NNPDF3.0NNLO	Sherpa 2.2.2	Default	NLO

Generators used are typically NLO and normalised with at least NLO (or higher order) cross-section predictions

$H \to c\bar{c}$ candidate selection

- Jets built with anti-k_T ($R = 0.4$) applied to calorimeter clusters
- Any muons within p_T dependent ΔR cone are used to correct the *signal jet* 4-vectors (recover energy in semi-leptonic b/c-hadron decays)
- At least two *central jets* required, one with $p_T > 45$ GeV
- Two highest p_T *central jets* (denoted the *signal jets*) form the $H \to c\bar{c}$ candidate
- p_T^V-dependent $\Delta R(\text{jet } 1, \text{jet } 2)$ requirement (see table $\to$)
- All non-signal jets must fail 70% b-jet efficiency b-tagging working point

central jets: $|\eta| < 2.5$, $p_T > 20$ GeV

forward jets: $2.5 < |\eta| < 4.5$, $p_T > 30$ GeV

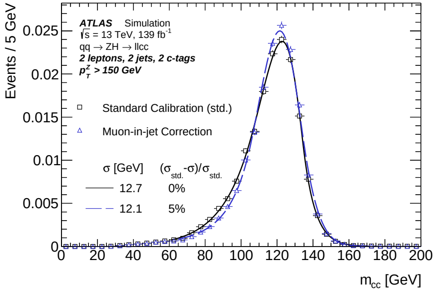

Invariant mass of $H \to c\bar{c}$ candidate, m_{cc}, is primary S/B discriminant

p_T^V	$\Delta R(\text{jet } 1, \text{jet } 2)$
$75 < p_T^V < 150$ GeV	≤ 2.3
$150 < p_T^V < 250$ GeV	≤ 1.6
$p_T^V > 250$ GeV	≤ 1.2

$VH, H \to c\bar{c}$ - 0 lepton channel

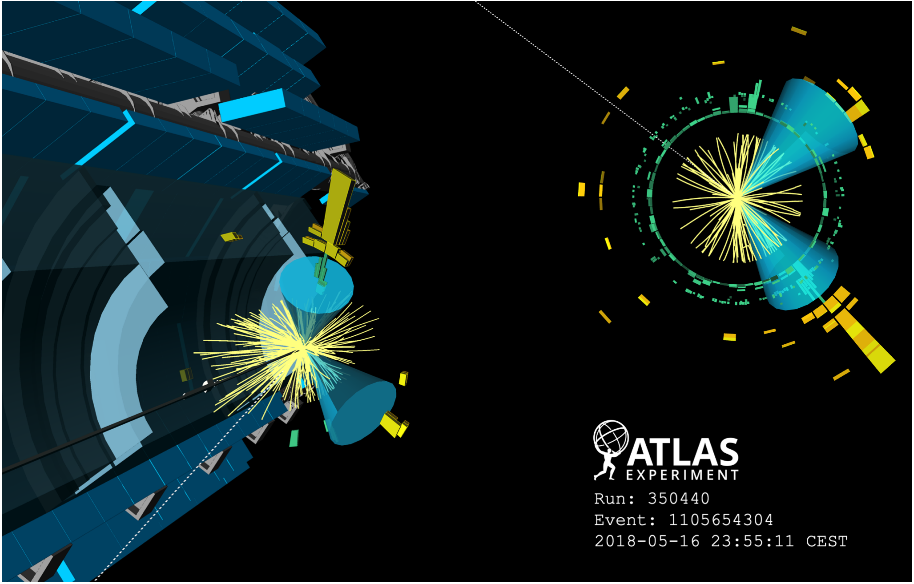

Candidate $Z(\nu\nu)H(c\bar{c})$ event with $E_{\mathrm{T}}^{\mathrm{miss}} = 155$ GeV and $m_{cc} = 125$ GeV

$VH, H \rightarrow c\bar{c}$ - 0 lepton channel

Event Selection and Categorisation

- Trigger events with $E_{\mathrm{T}}^{\mathrm{miss}}$ signature
- No leptons with $p_{\mathrm{T}} > 7$ GeV
- $E_{\mathrm{T}}^{\mathrm{miss}} > 150$ GeV
- Requirements on angular variables built from hadronic signatures and $E_{\mathrm{T}}^{\mathrm{miss}}$ to negate multi-jet background

Four Signal Regions	
1 c-tag, 2 jets	2 c-tags, 2 jets
1 c-tag, 3 jets	2 c-tags, 3 jets

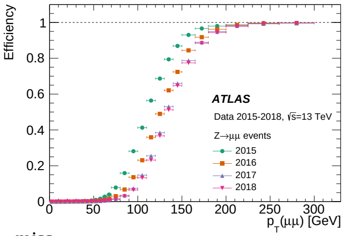

$E_{\mathrm{T}}^{\mathrm{miss}}$ trigger efficiency in data (JHEP 08 (2020) 80)

m_{cc} distribution for 0 lepton, 1 c-tag, 2 jet signal region ↓

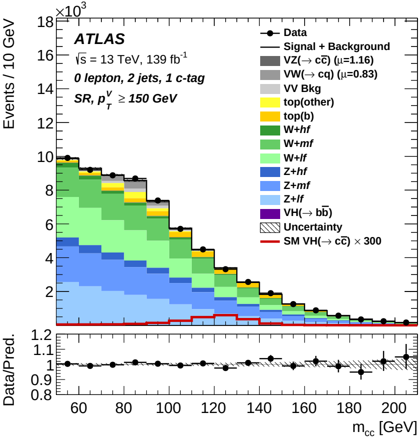

Complicated background dominated by W+jets, Z+jets and top quark processes, with sub-leading contributions from VW and VZ production

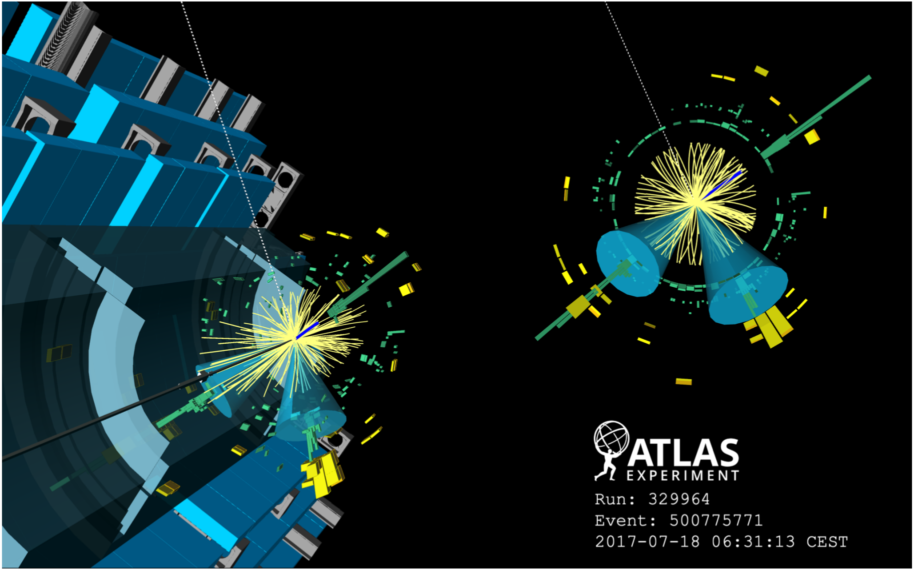

Candidate $W(e\nu)H(c\bar{c})$ event with $m_T^W = 62$ GeV and $m_{cc} = 124$ GeV

$VH, H \to c\bar{c}$ - 1 lepton channel

Event Selection and Categorisation

- Trigger events with single electron or $E_{\mathrm{T}}^{\mathrm{miss}}$ signatures (muon sub-channel)
- Exactly one isolated electron or muon with $p_{\mathrm{T}} > 27(25)$ GeV
- No further leptons with $p_{\mathrm{T}} > 7$ GeV
- $p_{\mathrm{T}}^{W} > 150$ GeV
- $m_{\mathrm{T}}^{W} < 120$ GeV and $E_{\mathrm{T}}^{\mathrm{miss}} > 30$ GeV (electron sub-channel only) to reduce multi-jet background

Four Signal Regions	
1 *c*-tag, 2 jets	2 *c*-tags, 2 jets
1 *c*-tag, 3 jets	2 *c*-tags, 3 jets

m_{cc} distribution for 1 lepton, 1 *c*-tag, 2 jet signal region ↓

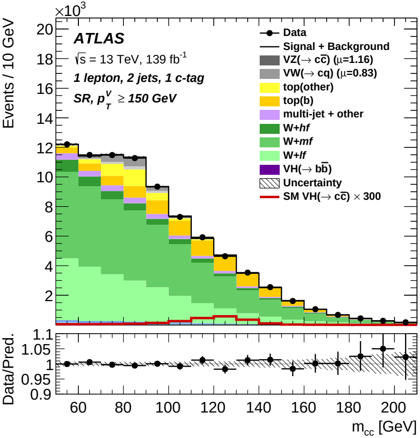

Background dominated by W+jets and top quark processes (primarily $t\bar{t}$ and Wt), with sub-leading contributions from VW and VZ production

Small contribution from multijet events modelled with data-driven method

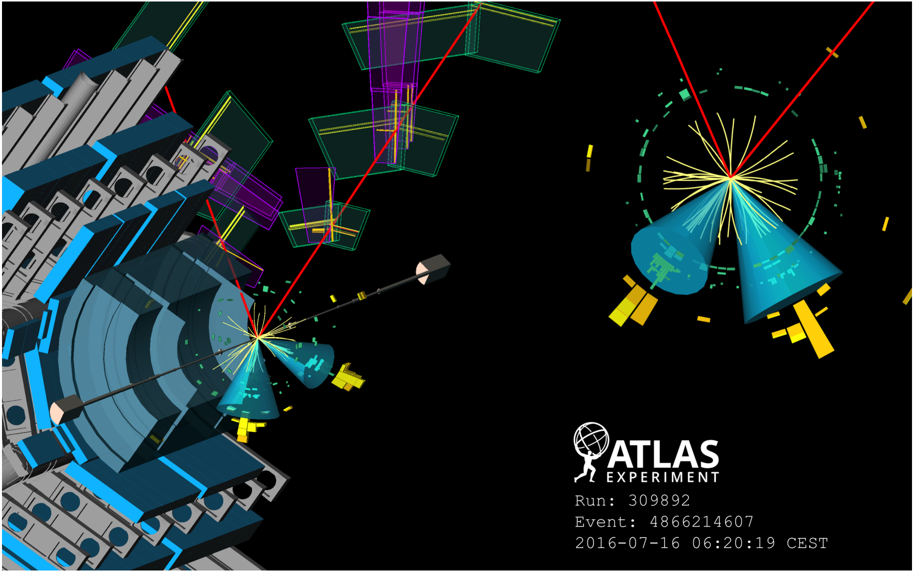

Candidate $Z(\mu^+\mu^-)H(c\bar{c})$ event with $m_{\mu^+\mu^-} = 92$ GeV and $m_{cc} = 123$ GeV

$VH, H \to c\bar{c}$ - 2 lepton channel

Event Selection and Categorisation

- Trigger events with single electron or single muon signatures
- Exactly two electrons or two muons, with $p_{\mathrm{T}} > 27(7)$ GeV required for the (sub-)leading lepton
- Require consistency with Z boson mass, $81 < m_{\ell\ell} < 101$ GeV
- $p_{\mathrm{T}}^{Z} > 75$ GeV

Eight Signal Regions	
$75 < p_{\mathrm{T}}^{Z} < 150$ GeV ("low p_{T}^{Z}")	
1 c-tag, 2 jets	2 c-tags, 2 jets
1 c-tag, ≥ 3 jets	2 c-tags, ≥ 3 jets
$p_{\mathrm{T}}^{Z} > 150$ GeV ("high p_{T}^{Z}")	
1 c-tag, 2 jets	2 c-tags, 2 jets
1 c-tag, ≥ 3 jets	2 c-tags, ≥ 3 jets

m_{cc} distribution for 2 lepton, 1 c-tag, 2 jet, high p_{T}^{Z} signal region ↓

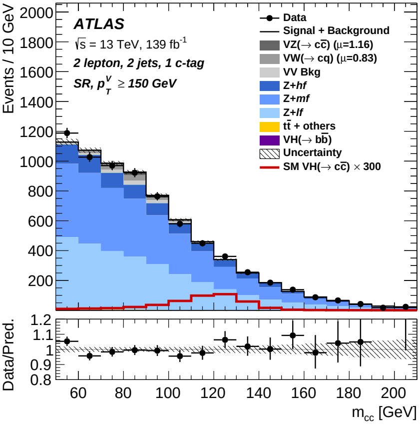

Background entirely dominated by Z+jets, with sub-leading contributions from VW and VZ production along with top quark processes in the low p_{T}^{Z} categories

$VH, H \to c\bar{c}$ - Control Regions

The complicated background composition calls for three classes of dedicated control regions (CR) to provide data-driven constraints on background modelling:

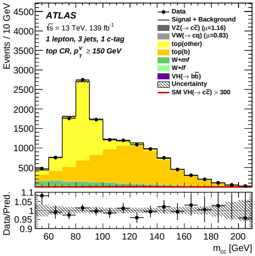

1) Top CRs to constrain modelling of top quark processes

- **0/1 lepton** - Invert b-tag veto in 1 c-tag, 3-jet events
- **2 lepton** - $e^{\pm}\mu^{\mp}$ events with 1 c-tag

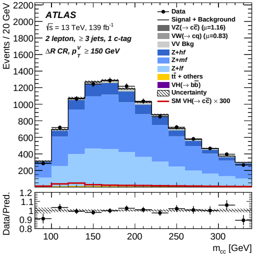

2) ΔR_{jj} CRs to constrain modelling of the W/Z+jets

- Events with ΔR_{jj} above nominal selection criteria, up to $\Delta R_{jj} < 2.5$

3) 0 c-tag CRs to constrain normalisation of W/Z+jets light flavour component

- Events in **1 and 2 lepton channels** where neither signal jet is c-tagged and any non-signal jets must fail the b-tagging requirement

$VH, H \to c\bar{c}$ - Statistical Analysis

Binned likelihood fit to the m_{cc} distributions of 16 SRs and 28 CRs used to quantify the presence/absence of a statistically significant $VH, H \to c\bar{c}$ signal

- **Di-boson** processes $VW(cq)$ and $VZ(c\bar{c})$ provide **in-situ validation channels**
- 3 parameters of interest: signal strengths for $VH(c\bar{c})$, $VW(cq)$ and $VZ(c\bar{c})$
- Experimental, signal / background modelling and MC statistical uncertainties implemented as nuisance parameters in the likelihood fit

↓ m_{cc} distributions for high purity 2 c-tag, 2 jet categories for 0, 1 and 2 lepton channels ↓

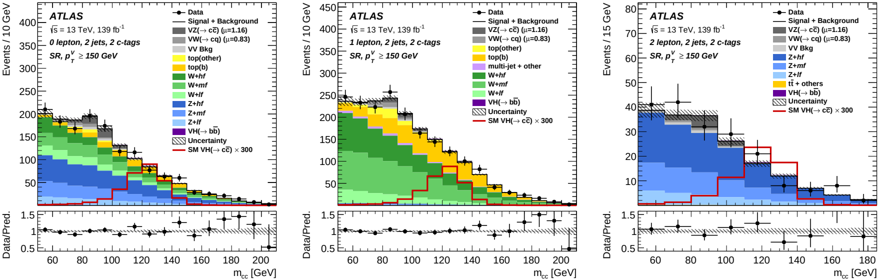

Categorisation and statistical model designed to maximise constraints from data and minimise reliance on MC simulation for background modelling

$VH, H \to c\bar{c}$ - Signal and Background Modelling Uncertainties

Floating background normalisation parameters determine the main background normalisations from the data itself:

- Three separate flavour component parameters each for $W+$ **jets** and $Z+$ **jets** (six in total)
- Three separate parameters for **top quark processes**, 0 and 1 lepton (with/without a b-quark), 2 lepton

$$\text{hf} = \{bb, cc\},\ \text{mf} = \{bl, cl, bc\},\ \text{lf} = \{ll, \tau X\}$$

For each signal and background processes, four categories of uncertainty are considered:

- **Cross-section and acceptance uncertainties** (where a floating normalisation parameter is not used)
- **Flavour or process composition uncertainties**
- **Inter-category relative normalisation uncertainties**
- m_{cc} shape uncertainties

Each uncertainty is estimated from theory uncertainties associated with cross-section / branching fraction predictions and / or alternative MC generator samples

$VH(\to b\bar{b})$	
$WH(\to b\bar{b})$ normalisation	27%
$ZH(\to b\bar{b})$ normalisation	25%
Diboson	
$WW/ZZ/WZ$ acceptance	10%/5%/12%
p_T^V acceptance	4%
N_{jet} acceptance	7%–11%
$Z+$jets	
$Z+hf$ normalisation	Floating
$Z+mf$ normalisation	Floating
$Z+lf$ normalisation	Floating
$Z+bb$ to $Z+cc$ ratio	20%
$Z+bl$ to $Z+cl$ ratio	18%
$Z+bc$ to $Z+cl$ ratio	6%
p_T^V acceptance	1%–8%
N_{jet} acceptance	10%–37%
High-ΔR CR to SR	12%–37%
0- to 2-lepton ratio	4%–5%
$W+$jets	
$W+hf$ normalisation	Floating
$W+mf$ normalisation	Floating
$W+lf$ normalisation	Floating
$W+bb$ to $W+cc$ ratio	4%–10%
$W+bl$ to $W+cl$ ratio	31%–32%
$W+bc$ to $W+cl$ ratio	31%–33%
$W\to\tau\nu(+c)$ to $W+cl$ ratio	11%
$W\to\tau\nu(+b)$ to $W+cl$ ratio	27%
$W\to\tau\nu(+l)$ to $W+l$ ratio	8%
N_{jet} acceptance	8%–14%
High-ΔR CR to SR	15%–29%
$W\to\tau\nu$ SR to high-ΔR CR ratio	5%–18%
0- to 1-lepton ratio	1%– 6%
Top quark (0- and 1-lepton)	
Top(b) normalisation	Floating
Top(other) normalisation	Floating
N_{jet} acceptance	7%–9%
0- to 1-lepton ratio	4%
SR/top CR acceptance ($t\bar{t}$)	9%
SR/top CR acceptance (Wt)	16%
Wt / $t\bar{t}$ ratio	10%
Top quark (2-lepton)	
Normalisation	Floating
Multi-jet (1-lepton)	
Normalisation	20%–100%

$VH, H \to c\bar{c}$ - "Philosophy" of fit model design

0 lepton →

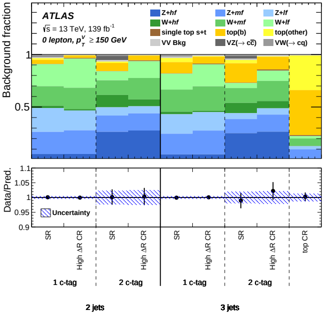

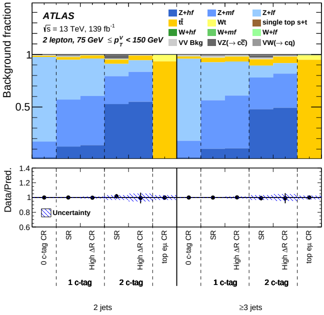

← 2 lepton (low p_T^Z)

1 lepton →

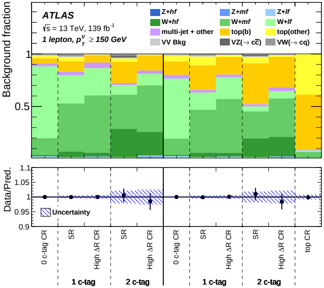

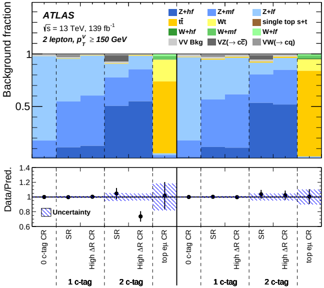

← 2 lepton (high p_T^Z)

Post-fit background subtracted m_{cc} distributions for the sum of all SRs help to visualise the sensitivity of the analysis to the three processes of interest:

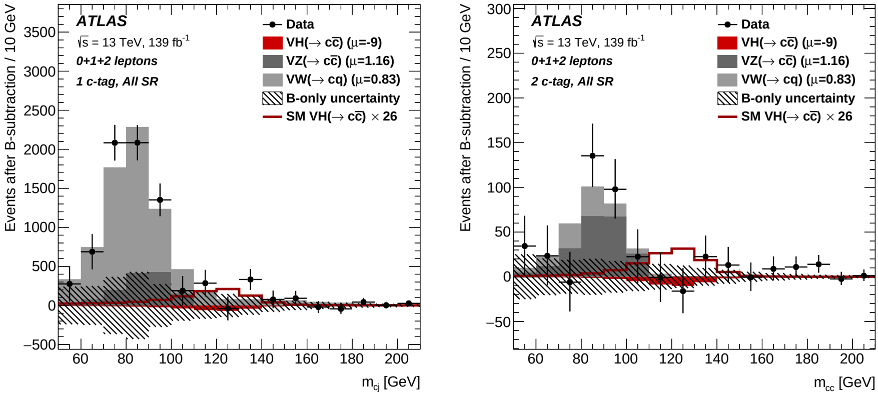

1 c-tag (left) categories drive sensitivity to $VW(cq)$, while the 2 c-tag categories (right) provide most sensitivity to $VZ(c\bar{c})$ and $VH(c\bar{c})$

VH, $H \to c\bar{c}$ - Results of likelihood fit

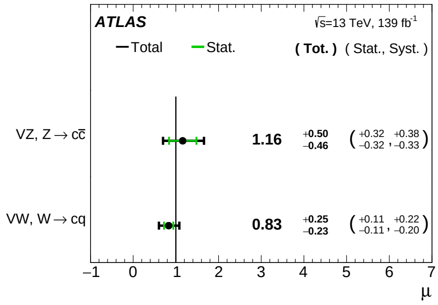

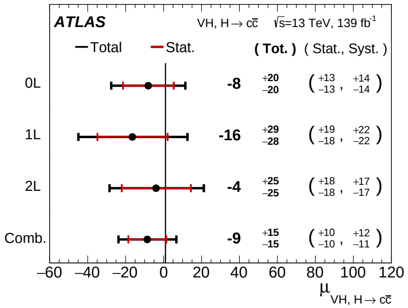

- ***VW(cq)*** **and** ***VZ(c$\bar{c}$)*** signal strength POIs found to be **consistent with SM predictions** → validation of the analysis methodology ✓
- *VH(c$\bar{c}$)* signal strength similarly consistent with zero and unity → **no evidence for signal at the SM rate**
- Probability of compatibility with SM (all 3 POI at unity) found to be 84%
- Measurements in **individual lepton channels very consistent** with combination

For baseline 3 POI fit, correlations coefficients between the POIs are found to be:

$VH(c\bar{c})$ vs. $VW(cq)$: +17%, $VH(c\bar{c})$ vs. $VZ(c\bar{c})$: +16%, $VW(cq)$ vs. $VZ(c\bar{c})$: -17%

The magnitude of statistical and systematic uncertainties are comparable for the $VH(c\bar{c})$ signal strength POI:

Source of uncertainty		$\mu_{VH(c\bar{c})}$	$\mu_{VW(cq)}$	$\mu_{VZ(c\bar{c})}$
Total		15.3	0.24	0.48
Statistical		10.0	0.11	0.32
Systematic		11.5	0.21	0.36
Statistical uncertainties				
Signal normalisation		7.8	0.05	0.23
Other normalisations		5.1	0.09	0.22
Theoretical and modelling uncertainties				
$VH(\to c\bar{c})$		2.1	< 0.01	0.01
$Z+$jets		7.0	0.05	0.17
Top quark		3.9	0.13	0.09
$W+$jets		3.0	0.05	0.11
Diboson		1.0	0.09	0.12
$VH(\to b\bar{b})$		0.8	< 0.01	0.01
Multi-jet		1.0	0.03	0.02
Simulation samples size		4.2	0.09	0.13
Experimental uncertainties				
Jets		2.8	0.06	0.13
Leptons		0.5	0.01	0.01
$E_{\mathrm{T}}^{\mathrm{miss}}$		0.2	0.01	0.01
Pile-up and luminosity		0.3	0.01	0.01
Flavour tagging	c-jets	1.6	0.05	0.16
	b-jets	1.1	0.01	0.03
	light-jets	0.4	0.01	0.06
	τ-jets	0.3	0.01	0.04
Truth-flavour tagging	ΔR correction	3.3	0.03	0.10
	Residual non-closure	1.7	0.03	0.10

Largest contributions to the total systematic uncertainty for $\mu_{VH(c\bar{c})}$ include:

- **Background modelling**, particularly for $Z+$jets
- Statistical uncertainty from **limited size of MC samples** available
- **Truth-flavour tagging** (though use of the method still provides a $\approx 10\%$ sensitivity gain)

Sensitivity to $VZ(c\bar{c})$ and $VW(cq)$ more clearly limited by systematic uncertainties, with hierarchy of contributions similar to that of $VH(c\bar{c})$

$VH, H \to c\bar{c}$ - Results

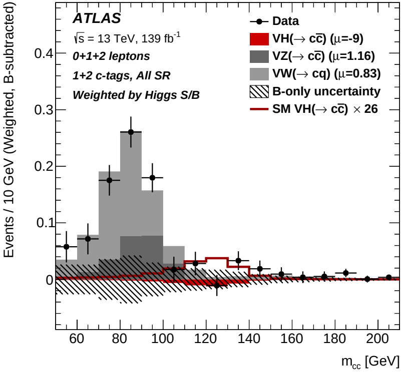

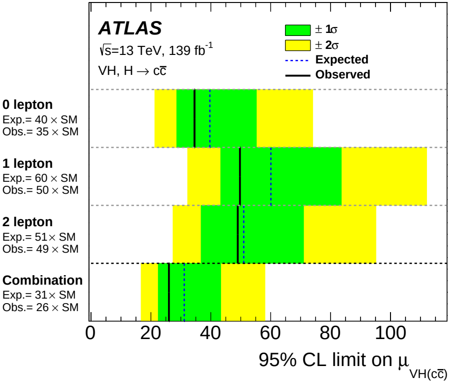

$VW(cq)$ observed (expected) significance 3.8 (4.6)σ

$VZ(c\bar{c})$ observed (expected) significance 2.6 (2.2)σ

Observed (expected) CLs limit on $\mu_{VH(c\bar{c})}$ is 26 (31^{+12}_{-8}) at 95% CL

$VH, H \to c\bar{c}$ - Interpretation within κ-framework

The result is interpreted in terms of the $Hc\bar{c}$ coupling based on the κ-framework†, inspired by the leading-order contributions to production and decay processes

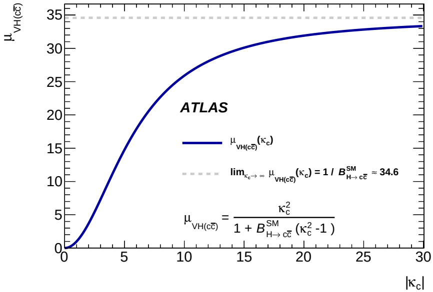

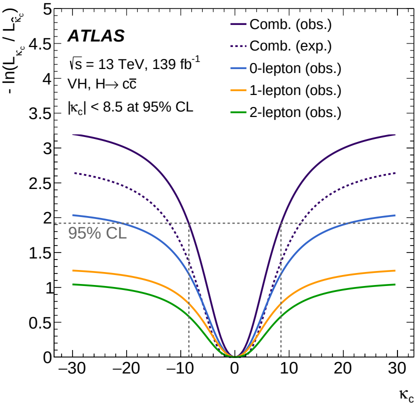

- Simple scenario considered where **only Higgs boson decay is parameterised** in terms of $\kappa_c = y_c / y_c^{SM}$
- All other couplings remain fixed to their SM values, no BSM particle contributions to Γ_H considered

✓ **Easy to understand** ✗ **Sensitive to assumptions on the Higgs total width Γ_H**

Observed (expected) constraint of $|\kappa_c| < 8.5\,(12.4)$ at 95% CL

† For more details, see LHC Higgs Cross Section Working Group Yellow Report 3 and Yellow Report 4

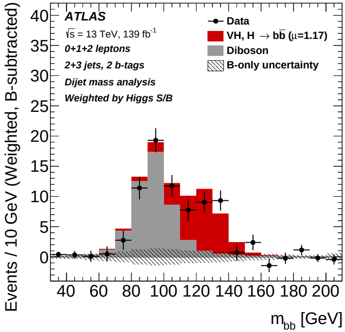

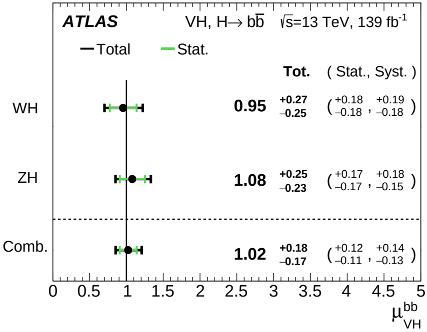

The careful design of the $VH, H \to c\bar{c}$ flavour tagging strategy allows for a straightforward combination with the ATLAS $VH, H \to b\bar{b}$ (resolved) analysis

- The signal regions of the two analyses are entirely orthogonal
- A combined analysis allows correlations in the signal strength coupling parameterisations (via Γ_H and σ_{VH}) between the two processes to be exploited

Such a combination has the power to derive more comprehensive and less model-dependent constraints on the $Hc\bar{c}$ and $Hb\bar{b}$ couplings

For more details on the ATLAS $VH, H \to b\bar{b}$ (resolved channel) analysis see: Eur. Phys. J. C 81 (2021) 178

At the SM rates, $VH, H \to b\bar{b}$ contributions to the $VH, H \to c\bar{c}$ signal regions (left) are 2(8)$\times$ the $VH, H \to c\bar{c}$ contributions in the 2(1) c-tag regions

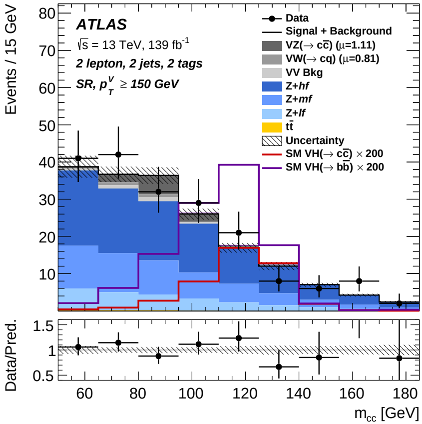

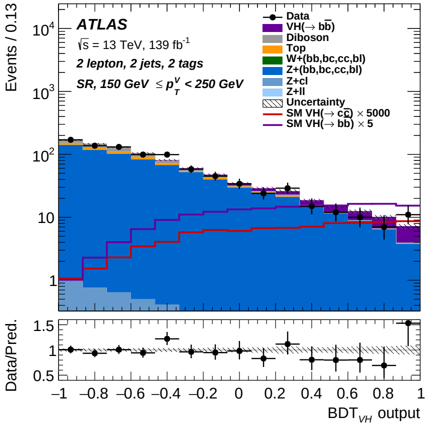

However, $VH, H \to c\bar{c}$ contributions to the $VH, H \to b\bar{b}$ signal regions (right) are very small (note the factor of 1000!)

Combination Procedure

- **Experimental systematic uncertainties** common to both analyses are treated as **correlated** (except $b/c-$tagging, due to differing calibration procedures)
- **Background modelling uncertainties and normalisation parameters** are treated as **uncorrelated** between the two analyses
- The alternative choice of correlating background normalisations was verifed to have no impact on the results

Combined Result

$$\mu_{VH(c\bar{c})} = -9 \pm 10\,(\text{stat.}) \pm 11\,(\text{syst.})$$

$$\mu_{VH(b\bar{b})} = 1.06 \pm 0.12\,(\text{stat.})^{+0.15}_{-0.13}\,(\text{syst.})$$

- Consistent with results of the individual analyses
- Correlation coefficient between two parameters is -12%

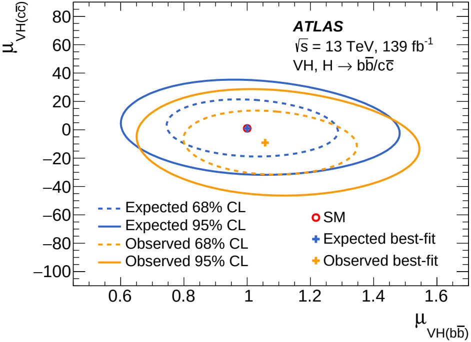

The $VH(b\bar{b})$ and $VH(c\bar{c})$ signal strengths are parameterised in terms of κ_b and κ_c, for both VH production and Higgs boson decay

- Fix other couplings to SM values, only SM production / decay channels considered

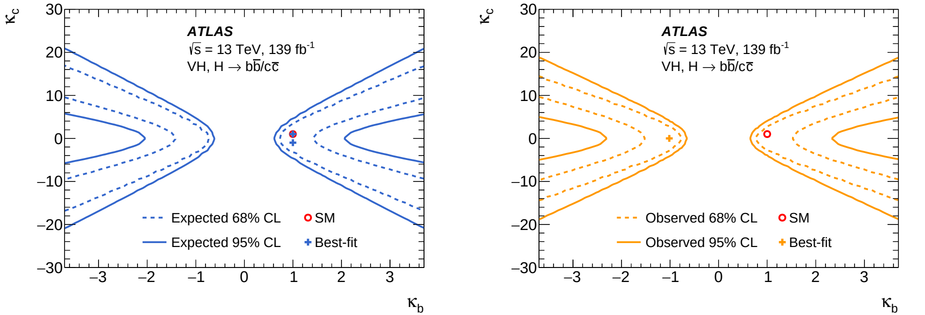

↑ **Expected and observed constraints in the κ_b vs. κ_c plane from combined profile-likelihood scan, best fit value is $(\kappa_b, \kappa_c) = (-1.02, 0)$**

- Only b-quark (not c-quark) loop contributions to $gg \to ZH$ parameterised, leading to small likelihood asymmetry in the κ_b direction which is absent for κ_c
- Log-likelihood difference between $(\kappa_b, \kappa_c) = (\{-1.02, +1.02\}, 0)$ is 0.02

For more details on the parameterisation, see ATLAS-CONF-2021-053

The $VH, H \to b\bar{b}/c\bar{c}$ signal strengths can also be parameterised in terms of the ratio of coupling modifiers κ_c/κ_b

- Ratio insensitive to Γ_H, no assumptions on decays to BSM particles required
- Profile likelihood scan of the ratio κ_c/κ_b is performed, with κ_b treated as a free parameter $\to$

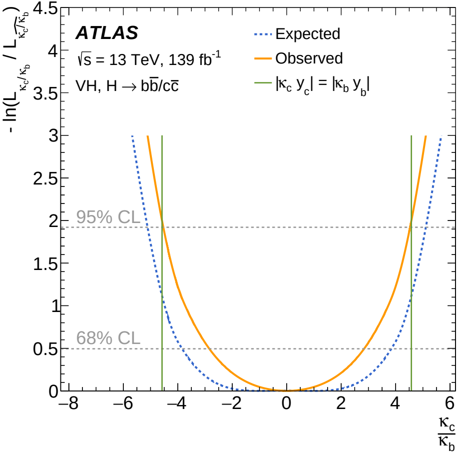

Observed (expected) constraint of $|\kappa_c/\kappa_b| < 4.5\,(5.1)$ at 95% CL

Observed constraint is smaller than the ratio of the b-quark and c-quark masses $m_b/m_c = 4.578 \pm 0.008$ [Phys. Rev. D 98 (2018) 054517 (from lattice QCD)]

Experimental confirmation that the Higgs boson's coupling to the charm quark is weaker than its coupling to the bottom quark!

Prospects for the $VH, H \to c\bar{c}/b\bar{b}$ analyses at the HL-LHC are assessed based on an extrapolation of the sensitivity of the existing Run 2 analyses:

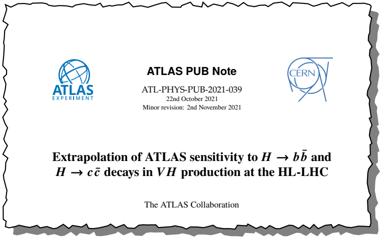
ATLAS PUB Note
ATL-PHYS-PUB-2021-039
22nd October 2021
Minor revision: 2nd November 2021

Extrapolation of ATLAS sensitivity to $H \to b\bar{b}$ and $H \to c\bar{c}$ decays in VH production at the HL-LHC

The ATLAS Collaboration

ATL-PHYS-PUB-2021-039

Uncertainties	Scale Factor
$E_{\mathrm{T}}^{\mathrm{miss}}$	0.5
Lepton	1
Jet	1
Flavour tagging c-, b- and τ-jets	0.5
Flavour tagging light-jets (MV2c10 in $VH(bb)$)	0.5
Flavour tagging light-jets (DL1 in $VH(cc)$)	1.0
Luminosity	0.58
Signal modelling	0.5
Background modelling	0.5
MC statistics	0
Truth-tagging uncertainties ($VH, H \to c\bar{c}$ only)	0

↑ Extrapolation uncertainty scale factors ↑

- Signal and background event yield predictions scaled from 139 fb^{-1} at $\sqrt{s} = 13$ TeV to 3000 fb^{-1} at $\sqrt{s} = 14$ TeV
- Experimental and theory uncertainties are based on Run 2 values, but scaled to account for reductions in their statistical components and potential improvements in analysis techniques associated with the larger dataset

Event selection, signal/background modelling and statistical analysis remain unchanged with respect to the Run 2 $VH, H \to c\bar{c}/b\bar{b}$ analyses described earlier

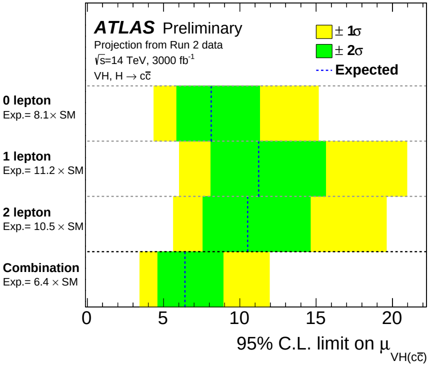

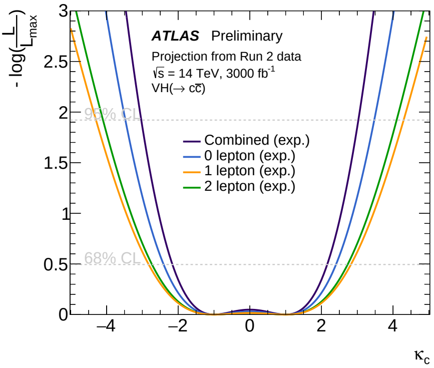

Expected limit on $VH(c\bar{c})$ signal strength of 6.4 at 95% CL

Expected constraint of $|\kappa_c| < 3.0$ at 95% CL

Extrapolating to a HL-LHC scenario with $3000\,\text{fb}^{-1}$ of $\sqrt{s} = 14$ TeV pp collision data, the existing $VH, H \to c\bar{c}$ analysis is not expected to reach SM sensitivity

Further innovation required in order to overcome systematic uncertainty limitations and improve sensitivity towards testing the SM prediction for the $Hc\bar{c}$!

Expected signal strength precision:

$$\mu_{VH(b\bar{b})} = 1.00 \pm 0.06$$

$$\mu_{VH(c\bar{c})} = 1.0 \pm 2.0\ (\text{stat.})^{+2.6}_{-2.5}\ (\text{syst.})$$

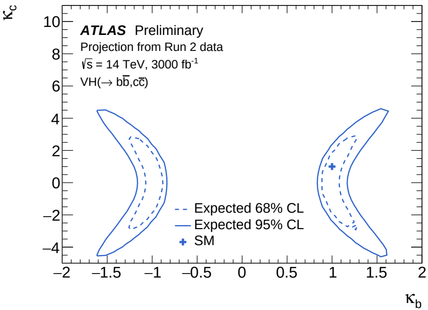

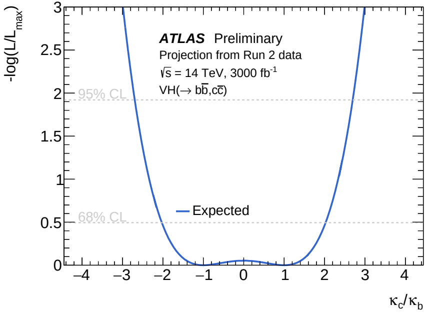

Expected constraint of $|\kappa_c/\kappa_b| < 2.7$ at 95% CL

Extrapolating to a HL-LHC scenario with $3000\,\text{fb}^{-1}$ of $\sqrt{s} = 14$ TeV *pp* collision data, the existing $VH, H \to c\bar{c}/b\bar{b}$ analyses fail to test SM prediction for κ_c/κ_b

⚠ **Assumes no new innovation in analysis design or b/c-tagging performance** ⚠

Many yet to be exploited opportunities exist, including designing the $VH, H \to c\bar{c}/b\bar{b}$ analyses in a more complementary manner!

The rate and kinematic features of inclusive Higgs boson production are sensitive to the $HQ\bar{Q}$ ($Q = c, b$) couplings in two main ways (+ many sub-leading effects):

- Loop-induced $gg \to H(g)$ production
- Quark-initiated production processes, such as $gQ \to HQ$ and $Q\bar{Q} \to Hg$
- **Modifications to the $HQ\bar{Q}$ couplings will alter the relative contributions** of these processes to inclusive Higgs boson production
- Results in **changes to cross-section and distortion of p_T^H** distribution

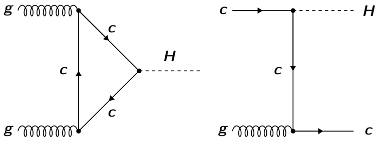

Examples of relevent Higgs boson production diagrams involving the $Hc\bar{c}$ coupling

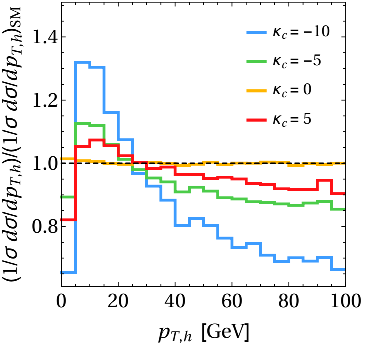

↑ **Shape effect on p_T^H associated with modifying y_c, from Phys. Rev. Lett. 118 (2017) 121801**

Shape of p_T^H is a relatively clean (exp. and th.) indirect probe of $y_{c,b}$, but modifications to rate are difficult to factorise from associated changes in Γ_H

Recently, the $H \to ZZ^* \to 4\ell^\dagger$ and $H \to \gamma\gamma^\ddagger$ fiducial differential cross-section measurements based on the complete 139 fb^{-1} ATLAS Run 2 dataset were statistically combined:

- Precision of the $H \to ZZ^* \to 4\ell$ and $H \to \gamma\gamma$ measurements is comparable
- Combined measurement of p_{T}^{H} remains **dominated by statistical uncertainties**
- Compatibility of combined p_{T}^{H} measurement with SM prediction is 20%

ATLAS-CONF-2022-002

†Eur. Phys. J. C 80 (2020) 941, ‡ arXiv:2202.00487

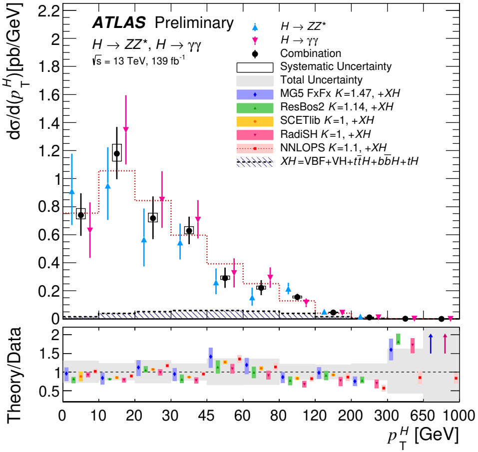

The individual and combined measurements are compared to a variety of theoretical predictions for $gg \to H$ production ↑

Only the measured shape of the p_T^H distribution is interpreted

- This removes assumptions associated with variations in branching fractions caused by $\kappa_{b,c}$ dependence of Γ_H

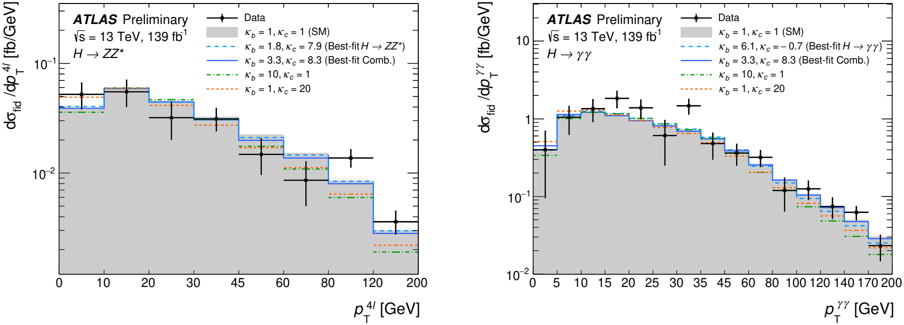

↑ **Expected fiducial p_T^H differential cross-section for a variety of κ_c and κ_b scenarios, with measurements overlaid**

- For example, large positive values of κ_c would reduce the cross-section at high p_T^H, while increasing it at low p_T^H (see $\kappa_c = 20$ scenario shown)

68% and 95% CL contours from $H \to ZZ^* \to 4\ell$, $H \to \gamma\gamma$ and their combination

↓ Expected ↓

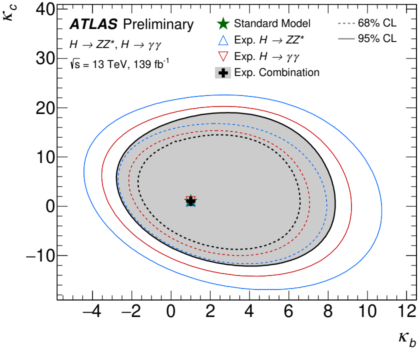

↓ Observed ↓

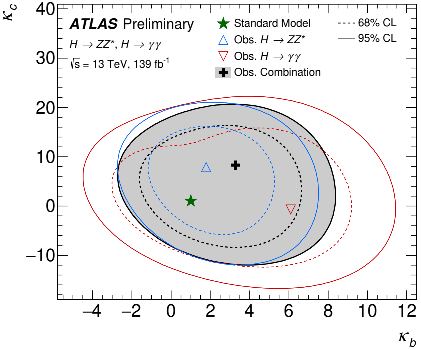

Combined expected constraint more stringent individual channels, though observed combined constraint is typically less stringent than that from $H \to ZZ^* \to 4\ell$

- Effect due to data fluctuations in some of the p_T^H bins, differing best fit values and double log-likelihood minimum associated with quadratic dependence of differential cross-section on $\kappa_{b,c}$

Log-likelihood scans for κ_b, determined while profiling κ_c

↓ Expected ↓

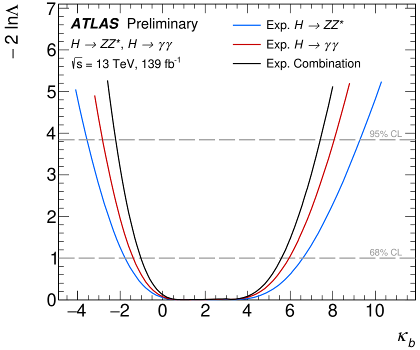

↓ Observed ↓

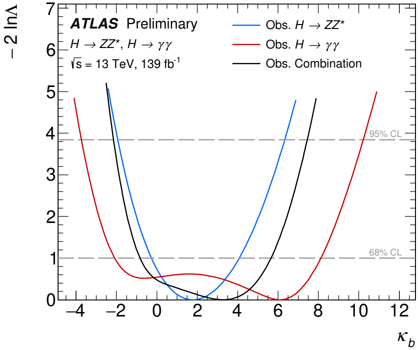

Channel	κ_b		
	Best Fit	95% Confidence Interval	
		Expected	Observed
$H \to ZZ^* \to 4\ell$	1.8	[-3.6,9.3]	[-1.9,6.3]
$H \to \gamma\gamma$	6.1	[-2.8,8.1]	[-3.7,10.2]
Combination	3.3	[-2.2,7.4]	**[-2.1,7.4]**

While expected combined constraint is weaker than that from $VH, H \to b\bar{b}$, it offers complementary sensitivity to the sign of κ_b

Log-likelihood scans for κ_c, determined while profiling κ_b

↓ **Expected** ↓

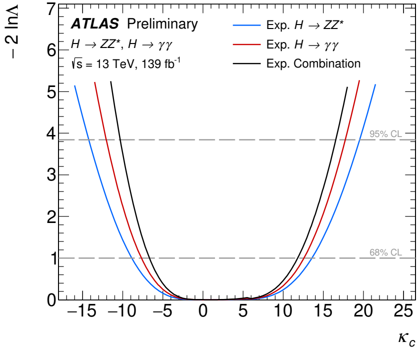

↓ **Observed** ↓

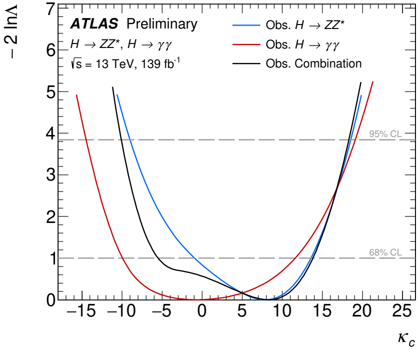

Channel	κ_c		
	Best Fit	95% Confidence Interval	
		Expected	Observed
$H \to ZZ^* \to 4\ell$	7.9	[-14.2,19.5]	[-9.0,18.5]
$H \to \gamma\gamma$	-0.7	[-12.0,-17.7]	[-14.5,19.1]
Combination	8.3	[-10.3,16.6]	**[-10.1,18.3]**

Expected combined constraint comparable to that of $VH, H \to c\bar{c}$ ($|\kappa_c| < 12.4$), yet subject to different assumptions and sources of uncertainty

Strong complementarity between the observed constraints in the κ_b vs. κ_c plane from interpreation of $VH, H \to b\bar{b}/c\bar{c}$ signal strengths and measurements of p_T^H from $H \to ZZ^* \to 4\ell$ and $H \to \gamma\gamma$

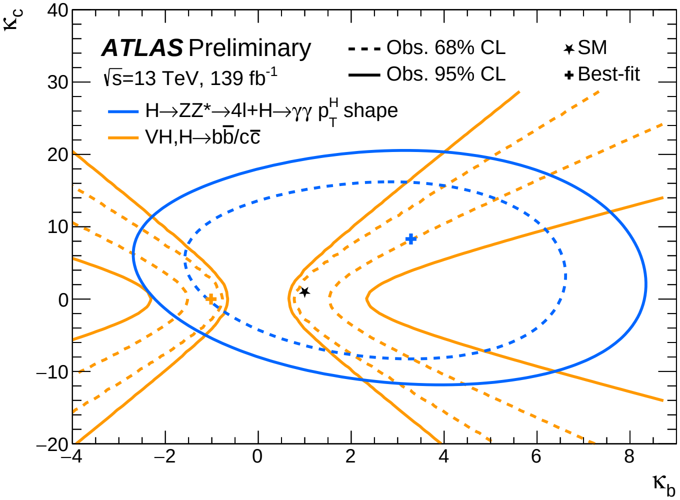

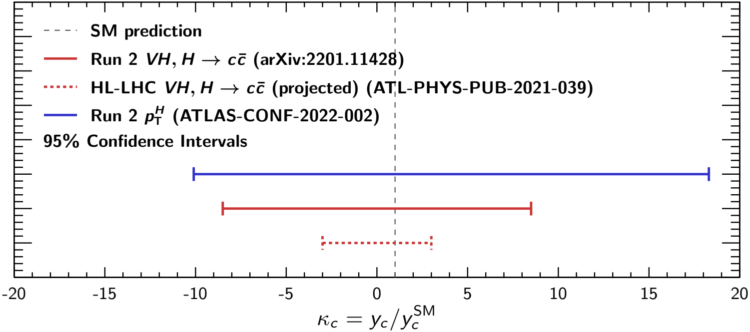

ATLAS is exploring the Higgs boson's coupling to the charm quark in a variety of channels, providing several complementary constraints!

- The combination of the $VH, H \to b\bar{b}/c\bar{c}$ analyses provide **experimental confirmation $Hc\bar{c}$ coupling is weaker than $Hb\bar{b}$ coupling**
- Existing analyses, extrapolated to HL-LHC conditions, will probe important BSM scenarios, but likely fall short of testing the SM predictions

Plenty of scope for exciting new developments to meet the challenge of testing the SM prediction and shedding light on the mystery of the fermion masses!

Additional Slides

Expected constraints in the κ_b vs. κ_c plane from interpreation of $VH, H \to b\bar{b}/c\bar{c}$ signal strengths and measurements of p_T^H from $H \to ZZ^* \to 4\ell$ and $H \to \gamma\gamma$

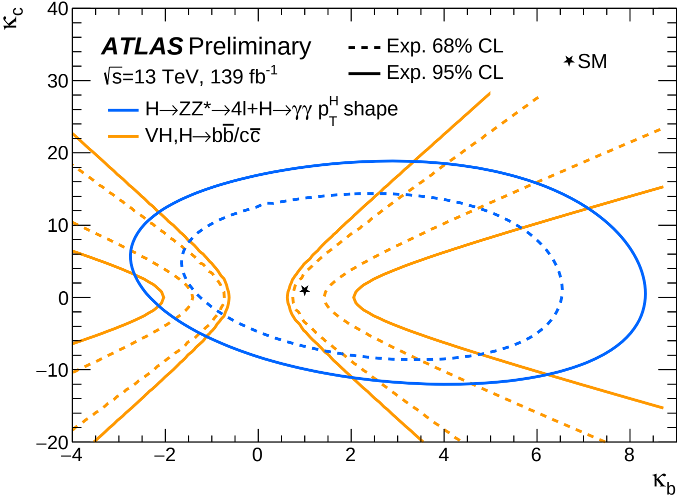

General purpose detector, well suited to studying heavy flavour jets

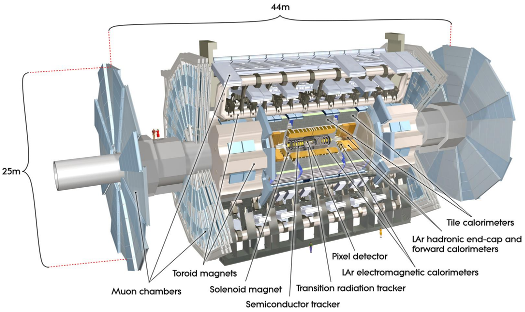

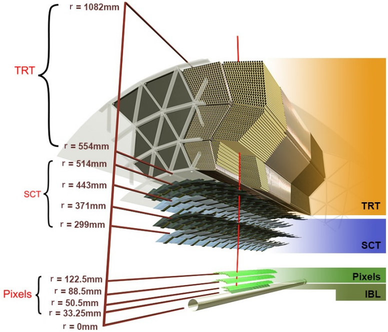

- **Inner Detector (ID):** Silicon Pixels and Strips (SCT) with Transition Radiation Tracker (TRT) $|\eta| < 2.5$ and (new for Run 2) Insertable B-Layer (IBL)
- **LAr EM Calorimeter:** Highly granular + longitudinally segmented (3-4 layers)
- **Had. Calorimeter:** Plastic scintillator tiles with iron absorber (LAr in fwd. region)
- **Muon Spectrometer (MS):** Triggering $|\eta| < 2.4$ and Precision Tracking $|\eta| < 2.7$
- **Jet Energy Resolution:** Typically $\sigma_E/E \approx 50\%/\sqrt{E(\text{ GeV})} \oplus 3\%$
- **Track IP Resolution:** $\sigma_{d_0} \approx 60\,\mu\text{m}$ and $\sigma_{z_0} \approx 140\,\mu\text{m}$ for $p_T = 1$ GeV (with IBL)

ATLAS has performed a search for $H \to J/\psi\,\gamma$ and $H \to \psi(2S)\,\gamma$ decays with $36\,\text{fb}^{-1}$ of 13 TeV pp collision data

- Analysis exploits the experimentally clean $\psi(nS) \to \mu^+\mu^-$ decay channels
- Dedicated photon + single muon triggers implemented to identify the distinctive event topology

Photon Selection

- "Tight" photon ID requirements
- Isolated in both tracker and calorimeter

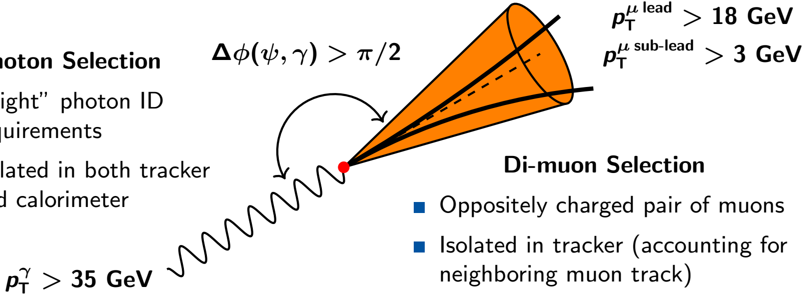

Di-muon Selection

- Oppositely charged pair of muons
- Isolated in tracker (accounting for neighboring muon track)
- $L_{xy}/\sigma_{L_{xy}} < 3$ to reject $b \to \psi(nS)$

Phys. Lett. B 786 (2018) 134 (arXiv:1807.00802)
(analogous rare Z decays and $\Upsilon(nS)\,\gamma$ channel also considered)

$VH, H \rightarrow c\bar{c}$ - Understanding the sensitivity, continued...

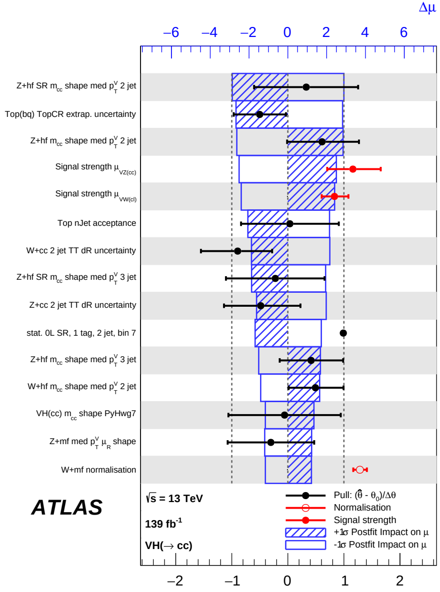

$VH, H \to c\bar{c}$ - Floating Normalisation Parameters

Background	p_T^V	Jets	Value
Top(b)			0.91 ± 0.06
Top(other)			0.94 ± 0.08
$t\bar{t}$ (2-lepton)	$p_T^V > 150$ GeV	2	0.76 ± 0.22
		3	0.96 ± 0.13
	$75 < p_T^V < 150$ GeV	2	1.08 ± 0.08
		3	1.06 ± 0.07
$W + hf$			1.16 ± 0.35
$W + mf$			1.28 ± 0.14
$W + lf$		2	1.02 ± 0.04
		3	0.97 ± 0.05
$Z + hf$	$p_T^V > 150$ GeV		1.19 ± 0.22
	$75 < p_T^V < 150$ GeV		1.25 ± 0.25
$Z + mf$	$p_T^V > 150$ GeV		1.10 ± 0.15
	$75 < p_T^V < 150$ GeV		1.11 ± 0.15
$Z + lf$	$p_T^V > 150$ GeV	2	1.07 ± 0.03
		3	1.08 ± 0.05
	$75 < p_T^V < 150$ GeV	2	1.12 ± 0.04
		3	1.07 ± 0.06

	0 lepton, $p_T^V > 150$			
	1 c-tag		2 c-tags	
	2 jets SR	3 jets SR	2 jets SR	3 jets SR
Z+lf	14 800 ± 2100	10 800 ± 1700	110 ± 30	81 ± 23
Z+mf	13 800 ± 1900	11 500 ± 1700	230 ± 40	195 ± 34
Z+hf	3500 ± 600	2900 ± 500	390 ± 60	370 ± 40
W+lf	13 700 ± 1700	8800 ± 1300	125 ± 26	69 ± 18
$W \to \tau\nu$	12 200 ± 1500	12 300 ± 1200	204 ± 31	205 ± 28
W+hf	1500 ± 400	1400 ± 400	170 ± 50	140 ± 40
Single top t-channel	163 ± 12	178 ± 18	1.8 ± 1.1	4.3 ± 1.1
Single top s-channel	22.2 ± 2.7	22 ± 1.9	0.88 ± 0.08	0.67 ± 0.07
top(b)	2570 ± 210	6230 ± 350	110 ± 10	269 ± 17
top(other)	1010 ± 110	2300 ± 200	19.2 ± 2.5	44 ± 5
$VZ(\to c\bar{c})$	380 ± 150	200 ± 100	57 ± 22	38 ± 14
$VW(\to cq)$	1100 ± 300	1000 ± 270	20 ± 5	19 ± 6
VV Bkg	740 ± 60	720 ± 70	20.5 ± 2.6	18.9 ± 2.5
$VH(\to b\bar{b})$	57 ± 12	41 ± 8	2.4 ± 0.5	1.6 ± 0.33
Total background	65 500 ± 280	58 300 ± 250	1468 ± 35	1450 ± 30
$VH(\to c\bar{c})$	−60 ± 110	−50 ± 90	−9 ± 15	−10 ± 10
$VH(\to c\bar{c})$ (expected)	8 ± 100	6 ± 80	1 ± 14	1 ± 10
S/B (expected)	4.06×10^{-4}	2.53×10^{-4}	2.53×10^{-3}	1.32×10^{-3}
Data	65490	58212	1462	1432

$VH, H \to c\bar{c}$ - Post-fit m_{cc} distributions: 0 lepton SRs

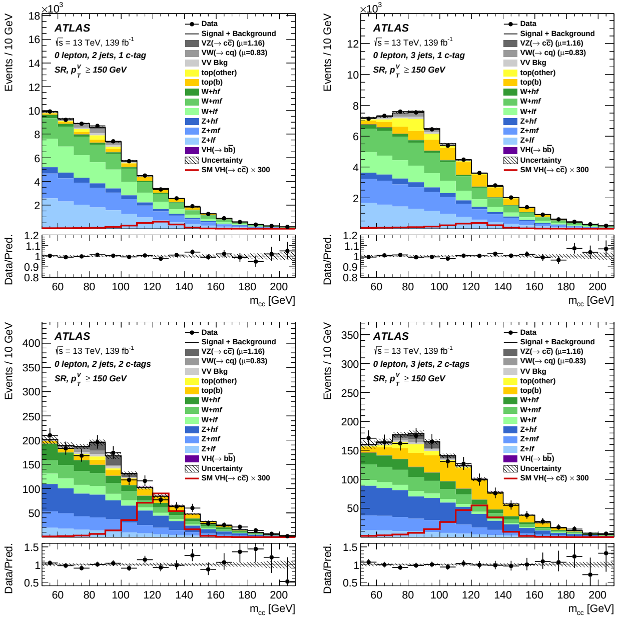

$VH, H \to c\bar{c}$ - Post-fit event composition: 1 lepton

	1 lepton, $p_T^V > 150$			
	1 c-tag		2 c-tags	
	2 jets SR	3 jets SR	2 jets SR	3 jets SR
Z+lf	1000 ± 100	860 ± 90	8 ± 2	10.7 ± 3.2
Z+mf	570 ± 70	640 ± 80	8.7 ± 2.5	11.4 ± 2.2
Z+hf	132 ± 13	132 ± 12	16 ± 4	19 ± 4
W+lf	22 000 ± 4000	14 200 ± 2700	170 ± 50	110 ± 30
$W \to \tau\nu$	38 000 ± 4000	35 000 ± 3000	620 ± 70	580 ± 60
W+hf	4300 ± 1200	3600 ± 1100	500 ± 100	400 ± 100
Single top t-channel	365 ± 32	500 ± 70	10.9 ± 1.1	17 ± 2
Single top s-channel	47 ± 4	40 ± 5	1.62 ± 0.16	0.93 ± 0.28
top(b)	8400 ± 600	20 000 ± 1000	380 ± 30	880 ± 50
top(other)	3200 ± 330	7200 ± 600	62 ± 8	130 ± 19
Multi-jet (μ)	1500 ± 800	600 ± 330	21 ± 17	7 ± 6
Multi-jet (e)	900 ± 400	950 ± 270	3 ± 2.9	22 ± 19
$VZ(\to c\bar{c})$	220 ± 90	180 ± 70	34 ± 13	28 ± 11
$VW(\to cq)$	1600 ± 400	1300 ± 400	29 ± 8	23 ± 6
VV Bkg	720 ± 70	760 ± 80	18.4 ± 2.4	20.8 ± 2.8
$VH(\to b\bar{b})$	56 ± 14	39 ± 11	2.3 ± 0.6	1.6 ± 0.4
Total background	84 020 ± 320	86 420 ± 350	1890 ± 40	2260 ± 40
$VH(\to c\bar{c})$	−60 ± 110	−50 ± 80	−8 ± 14	−10 ± 10
$VH(\to c\bar{c})$ (expected)	7 ± 100	5 ± 70	1 ± 13	1 ± 9
S/B (expected)	2.76×10^{-4}	1.38×10^{-4}	1.59×10^{-3}	6.26×10^{-4}
Data	83947	86316	1897	2277

$VH, H \to c\bar{c}$ - Post-fit m_{cc} distributions: 1 lepton SRs

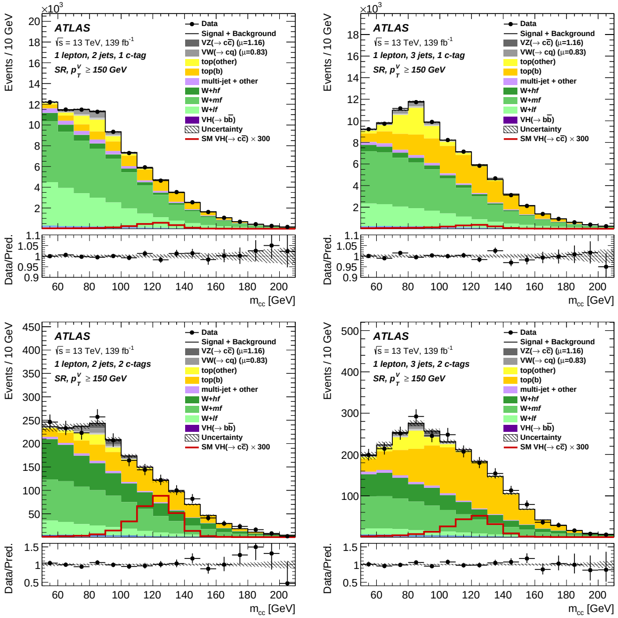

	2 lepton, $75 < p_T^V < 150$			
	1 c-tag		2 c-tags	
	2 jets SR	3 jets SR	2 jets SR	3 jets SR
Z+lf	16 000 ± 4000	14 400 ± 2700	130 ± 40	120 ± 30
Z+mf	19 000 ± 4000	18 400 ± 2700	300 ± 50	310 ± 40
Z+hf	5300 ± 800	4100 ± 600	590 ± 50	490 ± 50
W+lf	4.7 ± 1.3	12 ± 4	-	-
$W \to \tau\nu$	16 ± 11	18 ± 6	0.14 ± 0.03	-
W+hf	1.5 ± 0.4	1.85 ± 0.24	-	-
Single top Wt-channel	72 ± 6	86 ± 6	2.8 ± 0.7	2.32 ± 0.32
Single top t-channel	1.55 ± 0.34	2.8 ± 0.7	-	-
Single top s-channel	0.07 ± 0.03	0.2 ± 0.1	-	-
$t\bar{t}$	1080 ± 40	1690 ± 50	43.8 ± 3.4	61 ± 7
$VZ(\to c\bar{c})$	200 ± 80	140 ± 60	36 ± 16	23 ± 9
$VW(\to cq)$	380 ± 110	460 ± 140	6 ± 2	7.9 ± 2.5
VV Bkg	390 ± 30	530 ± 60	10 ± 1	13.9 ± 1.9
$VH(\to b\bar{b})$	24 ± 6	22 ± 7	0.94 ± 0.23	0.84 ± 0.26
Total background	42 460 ± 220	39 850 ± 240	1118 ± 32	1020 ± 29
$VH(\to c\bar{c})$	−20 ± 40	−30 ± 50	−3 ± 5	−3 ± 5
$VH(\to c\bar{c})$ (expected)	3 ± 40	3 ± 40	0.4 ± 5.2	0.3 ± 4.4
S/B (expected)	2.04×10^{-4}	1.58×10^{-4}	1.13×10^{-3}	7.73×10^{-3}
Data	42448	39808	1133	1009

$VH, H \to c\bar{c}$ - Post-fit m_{cc} distributions: 2 lepton "low p_T^Z" SRs

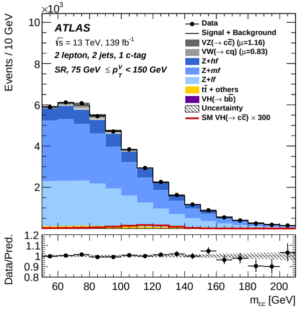

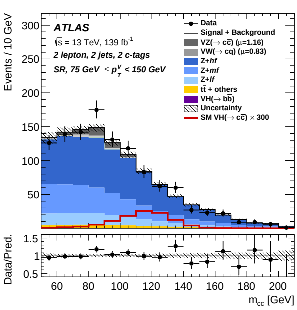

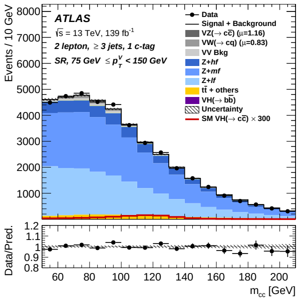

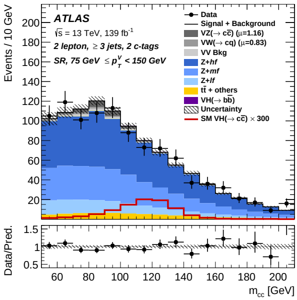

	2 lepton, $p_T^V > 150$			
	1 c-tag		2 c-tags	
	2 jets SR	3 jets SR	2 jets SR	3 jets SR
Z+lf	2900 ± 400	4100 ± 600	24 ± 5	33 ± 8
Z+mf	3100 ± 400	4900 ± 600	49 ± 7	79 ± 13
Z+hf	800 ± 150	1300 ± 200	92 ± 13	157 ± 19
W+lf	1.07 ± 0.28	4.1 ± 2.8	-	-
$W \to \tau\nu$	2.9 ± 0.5	1.5 ± 0.8	-	-
W+hf	0.05 ± 0.05	0.49 ± 0.15	-	0.02 ± 0.01
Single top Wt-channel	6.6 ± 0.7	15.7 ± 1.4	0.04 ± 0.03	0.28 ± 0.08
Single top t-channel	0.17 ± 0.02	0.2 ± 0.07	-	-
Single top s-channel	0.02 ± 0.01	-	-	-
$t\bar{t}$	22 ± 6	92 ± 12	0.87 ± 0.24	2.9 ± 0.4
$VZ(\to c\bar{c})$	67 ± 27	71 ± 28	11 ± 4	12 ± 5
$VW(\to cq)$	118 ± 35	200 ± 60	2.2 ± 0.7	3.5 ± 1.1
VV Bkg	110 ± 10	202 ± 26	3 ± 0.34	5 ± 1
$VH(\to b\bar{b})$	12.9 ± 3.2	16 ± 5	0.55 ± 0.14	0.6 ± 0.2
Total background	7100 ± 80	10 800 ± 100	182 ± 9	293 ± 13
$VH(\to c\bar{c})$	−13 ± 22	−18 ± 32	−1.7 ± 3.1	−2 ± 4
$VH(\to c\bar{c})$ (expected)	2 ± 20	2 ± 28	0.2 ± 2.9	0.3 ± 3.4
S/B (expected)	7.11×10^{-4}	4.78×10^{-4}	5.51×10^{-3}	3.36×10^{-3}
Data	7074	10812	189	302

$VH, H \to c\bar{c}$ - Post-fit m_{cc} distributions: 2 lepton “high p_T^Z” SRs

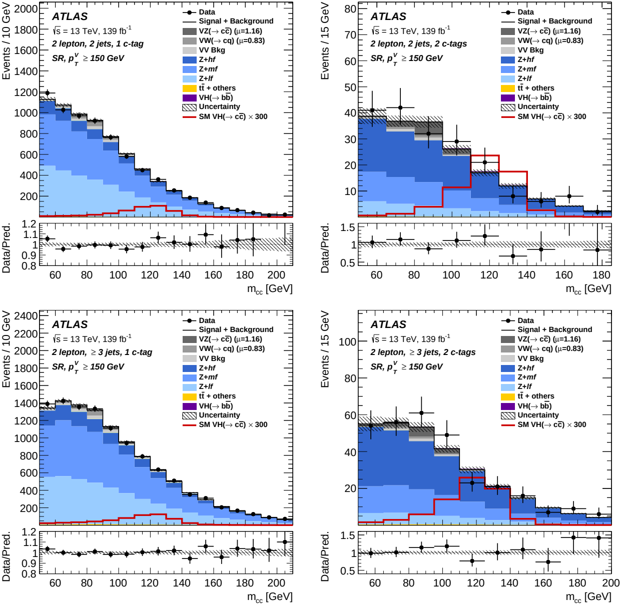

$VH, H \to c\bar{c}$ - Comparison with 36 fb^{-1} ATLAS analysis

"The improvements in this analysis relative to the previous ATLAS search for $ZH, H \to c\bar{c}$ are quantified by performing a fit in the 2-lepton channel to the 2015–2016 data, corresponding to 36 fb^{-1}. Using the same signal regions as the previous analysis a 36% improvement in the expected limit is found, with most of the improvement due to better flavour-tagging performance. After also including the new 2-lepton signal and control regions introduced in this analysis, a 43% improvement in the expected limit is found. Adding the full Run-2 dataset, along with the 0- and 1-lepton channels, the expected limit is improved by a factor of five in this analysis, relative to the previous ATLAS search."

From arXiv:2201.11428

Source of uncertainty		$\mu_{VH(c\bar{c})}$
Total		21.5
Statistical		16.2
Systematics		14.0
Statistical uncertainties		
Data statistics only		13.0
Floating normalisations		7.2
Theoretical and modelling uncertainties		
$VH(\to c\bar{c})$		2.1
Z+jets		7.7
Top-quark		5.6
W+jets		3.4
Diboson		0.8
$VH(\to b\bar{b})$		0.8
Multi-Jet		1.0
Simulation statistics		5.1
Experimental uncertainties		
Jets		3.7
Leptons		0.4
$E_{\mathrm{T}}^{\mathrm{miss}}$		0.5
Pile-up and luminosity		0.4
Flavour tagging	c-jets	2.3
	b-jets	1.2
	light-jets	0.7
	τ-jets	0.4
Truth-flavour tagging	ΔR correction	3.0
	Residual non-closure	1.4

Source of uncertainty		$\Delta\mu_{ZH}^{b\bar{b}}$	$\Delta\mu_{WH}^{b\bar{b}}$
Total		0.070	0.081
Statistical		0.034	0.039
Systematics		0.063	0.070
Statistical uncertainties			
Data statistics only		0.031	0.037
$t\bar{t}$ $e\mu$ control region		0.006	0.003
Floating normalisations		0.017	0.028
Theoretical and modelling uncertainties			
Signal		0.047	0.031
Z+jets		0.017	0.010
W+jets		0.004	0.022
single top		0.005	0.012
$t\bar{t}$		0.007	0.017
Diboson		0.020	0.027
Multi-Jet		< 0.001	0.001
Experimental uncertainties			
Jets		0.022	0.032
Leptons		0.006	0.011
$E_{\mathrm{T}}^{\mathrm{miss}}$		0.006	0.005
Pile-up and luminosity		0.009	0.009
Flavour tagging	b-jets	0.018	0.009
	c-jets	0.004	0.035
	light-jets	0.006	0.009

Source of uncertainty		$\Delta\mu_{VH}^{c\bar{c}}$
Total		3.21
Statistical		1.97
Systematics		2.53
Statistical uncertainties		
Data statistics only		1.59
Floating normalisations		0.95
Theoretical and modelling uncertainties		
$VH, H \to c\bar{c}$		0.27
Z+jets		1.77
Top-quark		0.96
W+jets		0.84
Diboson		0.34
$VH, H \to b\bar{b}$		0.29
Multi-Jet		0.09
Experimental uncertainties		
Jets		0.59
Leptons		0.20
$E_{\mathrm{T}}^{\mathrm{miss}}$		0.18
Pile-up and luminosity		0.19
Flavour tagging	c-jets	0.61
	b-jets	0.16
	light-jets	0.51
	τ-jets	0.19

$VH, H \to b\bar{b}$ - HL-LHC projection results

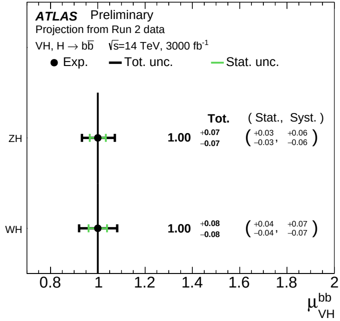

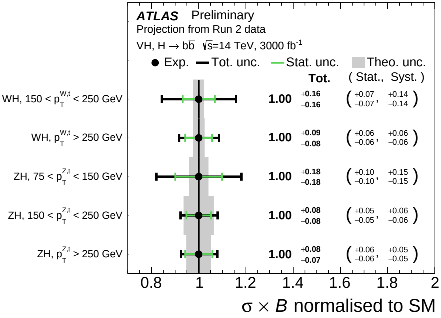

Source of uncertainty $p_T^{V,\,t}$	WH 150–250 GeV	WH ¿250 GeV	ZH 75–150 GeV	ZH 150–250 GeV	ZH ¿250 GeV
Total	0.157	0.085	0.180	0.079	0.077
Statistical	0.068	0.057	0.099	0.052	0.057
Systematics	0.141	0.063	0.150	0.059	0.051
Statistical uncertainties					
Data statistics only	0.063	0.054	0.082	0.059	0.056
$t\bar{t}$ $e\mu$ control region	0.018	0.004	0.050	0.012	0.004
Floating normalisations	0.063	0.023	0.080	0.030	0.019
Theoretical and modelling uncertainties					
Signal	0.020	0.027	0.023	0.028	0.036
Z+jets	0.023	0.009	0.103	0.019	0.019
W+jets	0.049	0.018	0.021	0.008	0.003
single top	0.043	0.009	0.015	0.012	0.005
$t\bar{t}$	0.062	0.018	0.024	0.008	0.008
Diboson	0.024	0.028	0.038	0.020	0.015
Multi-Jet	0.001	< 0.001	0.001	< 0.001	< 0.001
Experimental uncertainties					
Jets	0.076	0.031	0.083	0.031	0.019
Leptons	0.015	0.013	0.022	0.005	0.009
E_T^{miss}	0.058	0.012	0.058	0.008	0.007
Pile-up and luminosity	0.015	0.011	0.023	0.009	0.09
Flavour tagging b-jets	0.020	0.008	0.071	0.026	0.010
Flavour tagging c-jets	0.061	0.029	0.003	0.005	0.003
Flavour tagging light-jets	0.018	0.007	0.007	0.005	0.007

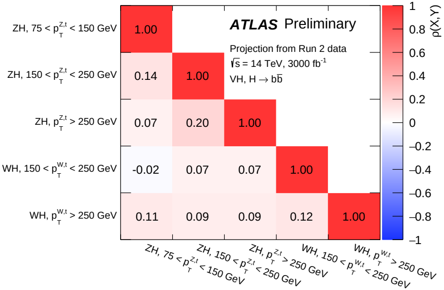

Production cross section	Loops	Main interference	Effective modifier	Resolved modifier
$\sigma(\text{ggF})$	✓	t–b	κ_g^2	$1.040\,\kappa_t^2 + 0.002\,\kappa_b^2 - 0.038\,\kappa_t\kappa_b - 0.005\,\kappa_t\kappa_c$
$\sigma(\text{VBF})$	-	-	-	$0.733\,\kappa_W^2 + 0.267\,\kappa_Z^2$
$\sigma(qq/qg \to ZH)$	-	-	-	κ_Z^2
$\sigma(gg \to ZH)$	✓	t–Z	$\kappa_{(ggZH)}$	$2.456\,\kappa_Z^2 + 0.456\,\kappa_t^2 - 1.903\,\kappa_Z\kappa_t$ $-0.011\,\kappa_Z\kappa_b + 0.003\,\kappa_t\kappa_b$
$\sigma(WH)$	-	-	-	κ_W^2
$\sigma(H)$	-	-	-	κ_t^2
$\sigma(tHW)$	-	t–W	-	$2.909\,\kappa_t^2 + 2.310\,\kappa_W^2 - 4.220\,\kappa_t\kappa_W$
$\sigma(tHq)$	-	t–W	-	$2.633\,\kappa_t^2 + 3.578\,\kappa_W^2 - 5.211\,\kappa_t\kappa_W$
$\sigma(H)$	-	-	-	κ_b^2
Partial decay width				
Γ^{bb}	-	-	-	κ_b^2
Γ^{WW}	-	-	-	κ_W^2
Γ^{gg}	✓	t–b	κ_g^2	$1.111\,\kappa_t^2 + 0.012\,\kappa_b^2 - 0.123\,\kappa_t\kappa_b$
$\Gamma^{\tau\tau}$	-	-	-	κ_τ^2
Γ^{ZZ}	-	-	-	κ_Z^2
Γ^{cc}	-	-	-	$\kappa_c^2\ (= \kappa_t^2)$
$\Gamma^{\gamma\gamma}$	✓	t–W	κ_γ^2	$1.589\,\kappa_W^2 + 0.072\,\kappa_t^2 - 0.674\,\kappa_W\kappa_t$ $+0.009\,\kappa_W\kappa_\tau + 0.008\,\kappa_W\kappa_b$ $-0.002\,\kappa_t\kappa_b - 0.002\,\kappa_t\kappa_\tau$
$\Gamma^{Z\gamma}$	✓	t–W	$\kappa_{(Z\gamma)}^2$	$1.118\,\kappa_W^2 - 0.125\,\kappa_W\kappa_t + 0.004\,\kappa_t^2 + 0.003\,\kappa_W\kappa_b$
Γ^{ss}	-	-	-	$\kappa_s^2\ (= \kappa_b^2)$
$\Gamma^{\mu\mu}$	-	-	-	κ_μ^2
Total width ($B_{\text{i.}} = B_{\text{u.}} = 0$)				
Γ_H	✓	-	κ_H^2	$0.581\,\kappa_b^2 + 0.215\,\kappa_W^2 + 0.082\,\kappa_g^2$ $+0.063\,\kappa_\tau^2 + 0.026\,\kappa_Z^2 + 0.029\,\kappa_c^2$ $+0.0023\,\kappa_\gamma^2 + 0.0015\,\kappa_{(Z\gamma)}^2$ $+0.0004\,\kappa_s^2 + 0.00022\,\kappa_\mu^2$

Figure from: ATLAS-CONF-2021-053

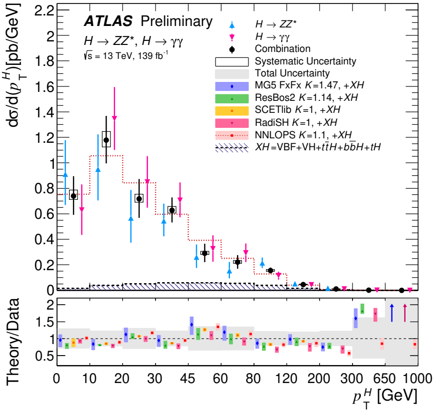

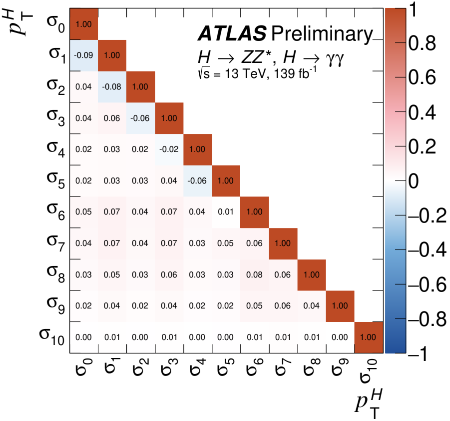

	σ_0	σ_1	σ_2	σ_3	σ_4	σ_5	σ_6	σ_7	σ_8	σ_9	σ_{10}
σ_0	1.00										
σ_1	-0.09	1.00									
σ_2	0.04	-0.08	1.00								
σ_3	0.04	0.06	-0.06	1.00							
σ_4	0.02	0.03	0.02	-0.02	1.00						
σ_5	0.02	0.03	0.03	0.04	-0.06	1.00					
σ_6	0.05	0.07	0.04	0.07	0.04	0.01	1.00				
σ_7	0.04	0.07	0.04	0.07	0.03	0.05	0.06	1.00			
σ_8	0.03	0.05	0.03	0.06	0.03	0.03	0.08	0.06	1.00		
σ_9	0.02	0.04	0.02	0.04	0.02	0.02	0.05	0.06	0.04	1.00	
σ_{10}	0.00	0.01	0.00	0.01	0.00	0.00	0.01	0.01	0.01	0.00	1.00

$H \to \gamma\gamma$

Photon and jet definitions	
Photons:	All photons except for those originating from hadron decay
	$p_T > 15$ GeV, $\lvert\eta\rvert < 1.37$ or $1.52 < \lvert\eta\rvert < 2.37$
	$E_T^{\mathrm{iso}}(\Delta R < 0.2, p_T > 1$ GeV, charged$) < 0.05\ E_T$
Jets:	$p_T > 30$ GeV, $\lvert y\rvert < 4.4$
Event selection	
Diphoton fiducial:	$N_\gamma \geq 2$, $p_T^{\gamma_1} > 0.35 m_{\gamma\gamma}$, $p_T^{\gamma_2} > 0.25 m_{\gamma\gamma}$
Mass window:	105 GeV $< m_{\gamma\gamma} <$ 160 GeV

Lepton and jet definitions	
Leptons	Dressed leptons not originating from hadrons or τ decay
	$p_T > 5$ GeV, $\lvert\eta\rvert < 2.7$
Jets	$p_T > 30$ GeV, $\lvert y\rvert < 4.4$
Lepton selection and pairing	
Lepton kinematics	p_T threshold for three leading leptons: $> 20, 15, 10$ GeV
Leading pair (m_{12})	SFOC lepton pair with smallest $\lvert m_Z - m_{\ell\ell}\rvert$
Subleading pair (m_{34})	remaining SFOC lepton pair with smallest $\lvert m_Z - m_{\ell\ell}\rvert$ as nominal.
Event selection (at most one quadruplet per event)	
Mass requirements	50 GeV$< m_{12} <$ 106 GeV and 12 GeV $< m_{34} <$ 115 GeV
Lepton separation	$\Delta R(\ell_i, \ell_j) > 0.1$
Lepton/Jet separation	$\Delta R(\ell_i, \mathrm{jet}) > 0.1$
J/ψ veto	$m(\ell_i, \ell_j) > 5$ GeV for all SFOC lepton pairs
Mass window	105 GeV $< m_{4\ell} <$ 160 GeV
If extra lepton with $p_T > 12$ GeV	Quadruplet with largest ggF matrix element value

$H \to ZZ^* \to 4\ell$